**The Thesis Committee for Mathew Ward Bissonnette**

**Certifies that this is the approved version of the following thesis:**

**Adaptive Vehicle Control by Combined DYC and FWS**

**APPROVED BY**

**SUPERVISING COMMITTEE:**

**Supervisor:**

Raul G. Longoria

Benito R. Fernandez

**Adaptive Vehicle Control by Combined DYC and FWS**


**by**

**Mathew Ward Bissonnette, B.S.**


**Thesis**

Presented to the Faculty of the Graduate School of

The University of Texas at Austin

in Partial Fulfillment

of the Requirements

for the Degree of


**Master of Science in Engineering**


**The University of Texas at Austin**

**May, 2014**

# Acknowledgements

# Abstract

## Adaptive Vehicle Control by Combined DYC and FWS

Mathew Ward Bissonnette, M.S.E.

The University of Texas at Austin, 2014

Supervisor: Raul G. Longoria

Vehicle stability is an important consideration in vehicle design. When driver intervention is insufficient, safety can be improved by the addition of vehicle stability control (VSC). Typical vehicle stability controllers are designed using a linearized vehicle model and an assumed set of parameters. However, some parameters like mass and inertial properties may not be constant between operations. To recover controller performance in the presence of unknown parameters, adaptive estimates can be developed. This thesis seeks to implement a model reference adaptive controller for yaw rate and side slip control and to evaluate any implementation issues that may arise. A linearized vehicle model is used for controller design via a Lyapunov approach and a combined front wheel steering (FWS) and direct yaw control (DYC) controller is developed. The combined FWS+DYC controller is tested in a low friction double lane change with initial parameter estimation error. The FWS+DYC controller was found to be robust to parameter changes, and the adaptive parameter estimates did not provide any noticeable improvement over the non-adaptive case. A four wheel steering (4WS) controller is developed by a similar approach and tested under the same conditions. Both controllers were found to be effective at stabilizing the vehicle. An unexpected

finding was that though the combined FWS+DYC controller was effective even in low friction conditions with parameter errors, the required motor torque was very large and oscillated rapidly. This was diminished through the addition of a low pass filter on the controller yaw moment output, but could not be removed entirely.

## Table of Contents

# List of Figures

# Chapter 1: Introduction

Vehicle stability is an important consideration in the design of passenger vehicles. In particular, handling stability has been a rich area of research for improving vehicle performance and safety. Near the tractive limits of the tires, vehicles may become unstable and difficult to control by the average driver. Vehicle stability control (VSC) prevents accidents by keeping vehicles under the control of the driver, even in extreme steering maneuvers. VSC is typically used to improve vehicle handling, but has also been applied to applications such as rollover prevention. For brevity, this thesis will only deal with the application of VSC for handling stability.

The typical controller is developed by assuming a set of vehicle parameters and designing around a simplified vehicle model. However, certain parameters may not be constant every time the vehicle is operated, and can depend on effects such as vehicle load or tire inflation [Wong, 2001]. In this thesis, a model reference adaptive controller (MRAC) is developed for tracking both yaw rate and side slip angle. The adaptive controller seeks to alleviate problems associated with uncertain parameters such as mass and inertial properties, geometric properties, and tire stiffness. A Lyapunov approach is pursued for controller development and for proof of convergence of the tracking error and boundedness of the parameter estimates. Additionally, a simple tire slip controller is implemented for producing the longitudinal tire forces required by the direct yaw control.

## 1.1 HISTORY OF DRIVER ASSISTANCE SYSTEMS

The average driver cannot detect road adhesion limits, nor vehicle stability factors [Zheng & Anwar, 2009]. Typically, drivers only have experience in stable handling maneuvers and cannot compensate well at the tractive limits. The usual driver response is overcompensation, which only exacerbates the problem. In situations like this, steering is the

most common cause of failure, and is the estimated cause in approximately 50% of accidents [Liebermann, et al., 2004], [van Zanten, 2002].

Loss of vehicle control can result in excessive skid or yaw rate. Excessive motion of either type can lead to side impacts or rollovers, accidents with a greatly increased risk of fatality. To alleviate this, a number of vehicle stability controllers have been developed. In studies using realistic driving simulators, VSC is shown to dramatically increase driver ability to maintain control of an otherwise unstable vehicle. In one study run by the University of Iowa, 34% more drivers maintained control with VSC than without [Liebermann, et al., 2004]. In addition to stabilizing a vehicle's motion, the controller must not give the driver the impression that their actions are being overridden or that the vehicle is considerably slowed down compared to the uncontrolled case.

Historically, there have been two approaches to stabilizing vehicle dynamics. The first is through augmented steering on either the front or rear wheels, depending on actuator availability. More recent approaches have concentrated on direct yaw control (DYC), which is achieved by differentially driving or braking the wheels to create a moment about the vehicle center. There have also been efforts to design combined systems that coordinate both augmented steering and DYC.

Early approaches to VSC concentrated solely on tracking a stable yaw rate. In 1992, a paper by Shibahata, et al. proposed the Beta Method of vehicle stability analysis [Furukawa & Abe, 1997], [Shibahata et al., 1992]. In this paper, it was noted that at high slip angles, the effect of steering is greatly diminished. Figure 1.1 [Lieberman, et al. 2004] shows the effect of side slip on the yaw moment generated by the tires for a given steering angle.
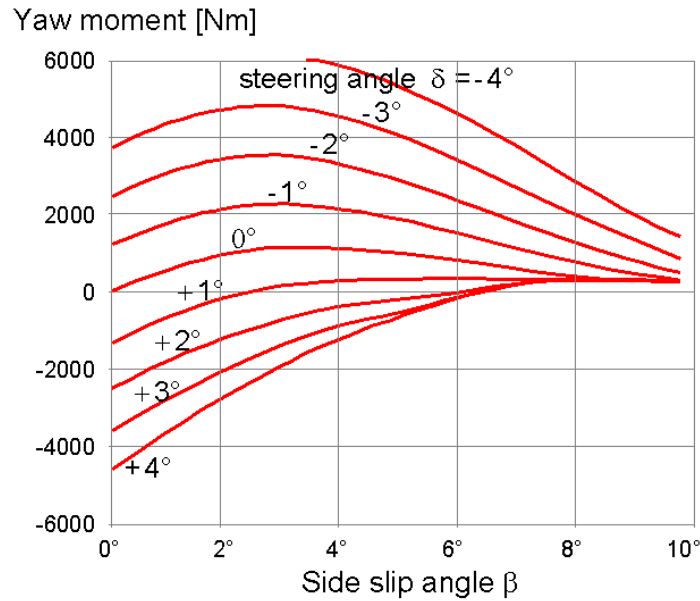
Figure 1.1 Influence of side slip angle on yaw moment produced by steering (dry asphalt)

The ability of the tires to generate a restoring moment when the vehicle is in a high-slip condition vanishes at about 12° on dry asphalt, 4° on packed snow, and 2° on ice [Liebermann, et al., 2004], [van Zanten, 2002].

Current VSC systems attempt to track a reference yaw rate while minimizing side slip. Control of the side slip angle via state feedback requires additional signal collection through expensive sensors. This has motivated the development of numerous observers for estimating side slip based on yaw rate and lateral acceleration [Ohara & Murakami, 2008], [Jianyong, et al., 2007], [Abe, et al., 2001]. Since development of such observers has been well documented by existing research, this paper will assume direct measurement of the system states.

### 1.1.1   Augmented Steering

The earliest VSC systems used an augmented steering approach made possible by the presence of a steer by wire system. Rather than allowing a driver to directly command the angle of the steered wheels via mechanical linkages, steering is accomplished through electromechanical actuators that receive inputs from the controller. In systems of this type, the driver's commanded steering angle, brake pressure, and commanded throttle are sent as inputs

3

to a stable reference model. The steering angle necessary to track this model is calculated by the controller and then applied to the wheels.

Numerous approaches have been proposed for development of FWS controllers. Ohara and Murakami have developed a FWS controller using a proportional derivative (PD) structure that, when coupled with a Luenberger observer for estimating disturbances and side slip, was shown to stabilize the vehicle even in the presence of an external disturbance torque [Ohara & Murakami, 2008]. Zheng and Anwar used a FWS controller to decouple the yaw rate and side slip via a full state feedback system with gain scheduling based on vehicle velocity [Zheng & Anwar, 2009]. Wang & Hsieh have expanded upon the basic idea of a FWS controller, and created a mass and inertia independent adaptive control law for yaw rate tracking [Wang & Hsieh, 2009]. Their work is discussed in greater detail later in this chapter. On vehicles equipped with both front and rear wheel steer-by-wire systems, four wheel steering has been shown to be a viable improvement over front wheel steering alone [Jianyong, et al., 2007], [Mokhiamar & Abe, 2002b], [Furukawa & Abe, 1997].

The augmented steering approach is attractive for its low cost and simplicity of implementation. However, steering is only effective below the saturation limits of the tire forces and fails in high side slip conditions. Once the vehicle side slip becomes too high, yaw moments generated by steering vanish and the controller fails to stabilize the vehicle. Figure 1.1 in the previous section demonstrates this phenomenon.

### 1.1.2   Direct Yaw Control

More recent systems seek to improve vehicle response through the use of yaw moments about the c.g. generated through differential driving or braking of the driven wheels. The addition of DYC has been shown to be an effective vehicle stability technique in a number of papers. Jianyong, et al. developed a combined rear wheel steering and DYC approach in an $H_\infty$ optimal controller designed for input/output constraints and disturbance rejection [Jianyong, et al., 2007]. Shino and Nagai utilized a combined feedforward/feedback control that

used DYC to drive the side slip angle to zero [Shino & Nagai, 2001]. Mirzaei used an LQ optimal controller to minimize the commanded yaw moment at the expense of acceptable ranges of tracking error [Mirzaei, 2010]. In these papers, and others, it is noted that direct yaw control provides superior performance at the tractive limits of the tires when compared to an augmented steering approach [Furukawa & Abe, 1997], [Mokhiamar & Abe, 2002a], [Mokhiamar & Abe, 2002b].

### 1.1.3   Improvement via Adaptive Control

In order to improve controller performance in the presence of uncertain parameters, a model reference adaptive controller (MRAC) is proposed. An adaptive FWS controller for yaw rate stabilization has previously been developed by researchers at The Ohio State University [Wang & Hsieh, 2009]. Their controller was developed to be independent of both mass and inertial properties, and was shown to be effective in a split-mu braking condition and a low friction double lane change. Their conclusions suggests that an adaptive controller that also accounts for unknown geometric parameters may be of value. Another adaptive FWS controller has been developed by the Ford Research and Advanced Engineering group. Their controller implements adaptive PI control with anti-windup compensators and pre-filtering of the system states, but assumes that the unknown parameters are constrained within certain known bounds [Kahveci, 2009].

This thesis seeks to answer the question of whether a feedback/feedforward construction of adaptive controller could be applied to a passenger vehicle using combined FWS and DYC. The controller is derived using the linear bicycle model and then validated using a nonlinear handling model. The system state and input matrices are taken to be constant, unknown parameters. These matrices include properties such as tire stiffness, vehicle geometry, and vehicle mass properties. The adaptive controller is proposed for tracking a stable reference signal for both yaw rate and side slip angle. A four wheel steering controller is also

developed for comparison. The controller follows the general structure shown below in Figure 1.2.
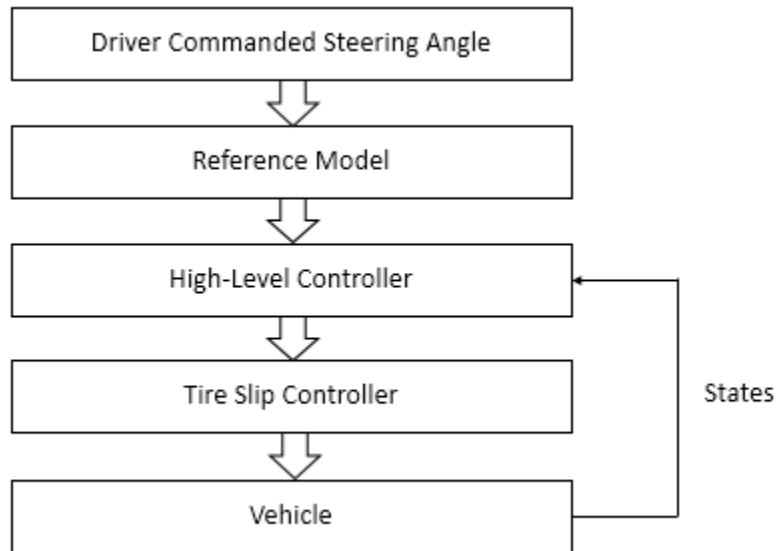


Figure 1.2 Controller hierarchy

This paper primarily focuses on the development of a high level controller, and a simple tire slip controller is included for completeness. Interested readers should look to [Wang & Longoria, 2006], [Liang, et al., 2009], [Canudas & Tsiotras, 1999], and [Hsiao, 2013] for a more in depth discussion of tire slip controllers.

**1.2 THESIS SCOPE AND ORGANIZATION**

The remainder of the thesis is organized as follows. In Chapter 2, the vehicle dynamics are discussed, including a review of tire models. Chapter 3 provides control theory background and details the development of a coordinated FWS and DYC controller via Lyapunov analysis. An adaptive control law is also proposed for estimation of the uncertain vehicle parameters. In Chapter 4, the controller is validated using a MatLab simulation of the full, nonlinear vehicle. Finally, Chapter 5 presents conclusions and proposed future work.

# Chapter 2: System Model

This chapter presents the derivation of the dynamic equations for the vehicle handling model. To simplify analysis, several simplifications have been made. Aerodynamic and friction loads are neglected, the vehicle is treated as a rigid body, and roll and dynamic load transfer effects are excluded. Section 2.1 shows the dynamic model for the nonlinear system. An overview of tire modeling is presented in section 2.2, and a detailed explanation of the chosen tire model is in section 2.2.1. A simplified, linear model that will be used for controller development is presented in section 2.3, and a historical background on directional stability follows. Finally, the reference model used in the tracking controller is developed in section 2.4.

## 2.1 NONLINEAR HANDLING MODEL

The equations of motion for a rigid body in 3D motion are given by the following differential equations, often referred to as the Euler equations.

$$\dot{p}_x = F_x - \Omega_y p_z + \Omega_z p_y \qquad (2.1)$$

$$\dot{p}_y = F_y - \Omega_z p_x + \Omega_x p_z \qquad (2.2)$$

$$\dot{p}_z = F_z - \Omega_x p_y + \Omega_y p_x \qquad (2.3)$$

$$\dot{h}_x = T_x - \Omega_y h_z + \Omega_z h_y \qquad (2.4)$$

$$\dot{h}_y = T_y - \Omega_z h_x + \Omega_x h_z \qquad (2.5)$$

$$\dot{h}_z = T_z - \Omega_x h_y + \Omega_y h_x \qquad (2.6)$$

Where $p_i$, $h_i$ represent the linear or rotational momenta for each of the reference axes in a body-fixed coordinate system, and $T_i$, $F_i$ are external torques or forces along the i-th axis. These equations are then applied to a vehicle handling model, shown below in Figure 2. [Jianyong, et al. 2007].
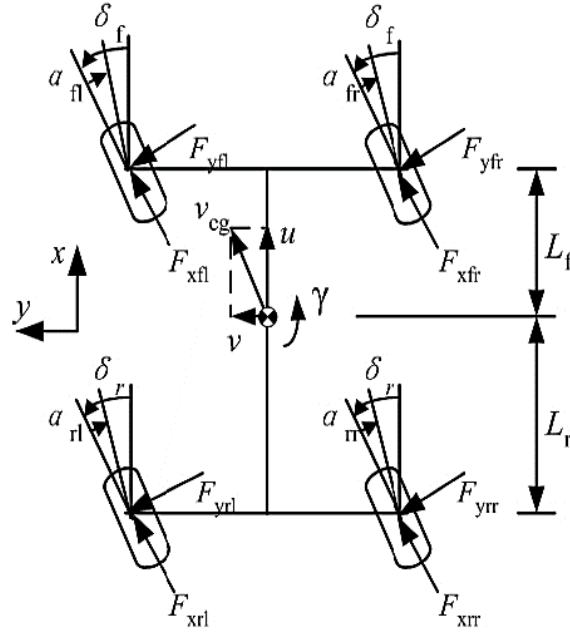
Figure 2.1 Four wheel vehicle model

In this model, suspension effects and load transfer are neglected. The equations of motion for this model are

$$\dot{V}_x = \frac{1}{m}\left[X_{fl} + X_{fr} + X_{rl} + X_{rr}\right] + V_y\Omega_z \qquad (2.7)$$

$$\dot{V}_y = \frac{1}{m}\left[Y_{fl} + Y_{fr} + Y_{rl} + Y_{rr}\right] - V_x\Omega_z \qquad (2.8)$$

$$\dot{\Omega}_z = \frac{1}{I_z}\left[L_f\left(Y_{fl} + Y_{fr}\right) - L_r(Y_{rl} + Y_{rr}) - 0.5b_f\left(X_{fl} - X_{fr}\right) - 0.5b_r(X_{rl} - X_{rr})\right] \qquad (2.9)$$

where $V_x$, $V_y$, and $\Omega_z$ are the body fixed longitudinal velocity, lateral velocity, and yaw rate of the vehicle. $X_{ij}$ and $Y_{ij}$ are the body fixed longitudinal and lateral forces developed by tire slip and slip angles. The subscripts i = f,r and j = r,l denote the corresponding front/rear and right/left tire. The forces $X_{ij}$ and $Y_{ij}$ are composed of the longitudinal and lateral forces on each tire, and are given by the following equations

8

$$X_{ij} = F_{xij} \cos(\delta_{ij}) - F_{yij}\sin(\delta_{ij})$$

(2.10)

$$Y_{ij} = F_{xij} \sin(\delta_{ij}) + F_{yij}\cos(\delta_{ij})$$

(2.11)

The tire forces are developed using the Pacejka Magic Formula

$$y(x) = D \sin\left[C \operatorname{atan}\{B\ x_{ij} - E(B\ x_{ij} - \operatorname{atan}(B\ x_{ij}))\}\right]$$

(2.12)

where y is either the lateral tire force with $x_{ij}$ the tire slip angle, or the longitudinal force with $x_{ij}$ the longitudinal wheel slip and B, C, D, and E are experimentally determined coefficients. The Pacjecka tire model and other tire models are discussed in further detail in section 2.2. The tire slip angle can be calculated for each wheel as follows

$$\alpha_{fl} = \delta_f - \operatorname{atan}\left(\frac{V_y + L_f\Omega_z}{V_x - 0.5b_f\Omega_z}\right)$$

(2.13)

$$\alpha_{fr} = \delta_f - \operatorname{atan}\left(\frac{V_y + L_f\Omega_z}{V_x + 0.5b_f\Omega_z}\right)$$

(2.14)

$$\alpha_{rl} = \delta_r - \operatorname{atan}\left(\frac{V_y - L_r\Omega_z}{V_x - 0.5b_r\Omega_z}\right)$$

(2.15)

$$\alpha_{rr} = \delta_r - \operatorname{atan}\left(\frac{V_y - L_r\Omega_z}{V_x + 0.5b_r\Omega_z}\right)$$

(2.16)

Additionally, the longitudinal slip for each tire is given by the following equation

$$\lambda_{ij} = \frac{R\omega - V_x}{\max(V_x, R\omega)}$$

(2.17)

## 2.2 TIRE MODELING

Tire behavior plays a large role in modeling vehicle handling performance. Since all control forces must be generated at the road/tire interface, an accurate tire model is required for a realistic controller validation. In a pneumatic tire, forces are generated by deformation of the tire carcass and sliding friction within the contact patch [Wong, 2001]. These two

9

phenomena are described in terms of the tire side slip angle and longitudinal slip, respectively. The side slip angle is the angle between the tire's heading and the tire velocity vector. The longitudinal slip is the ratio between the forward velocity of the tire and the linear velocity of the wheel at the contact patch. A longitudinal slip of 0% corresponds to pure rolling, while 100% corresponds to a pure slip condition. A typical steady state force/slip profile is shown below in Figure 2.2. The tire forces increase linearly within a small region centered about the origin, but decreases beyond a certain peak value.
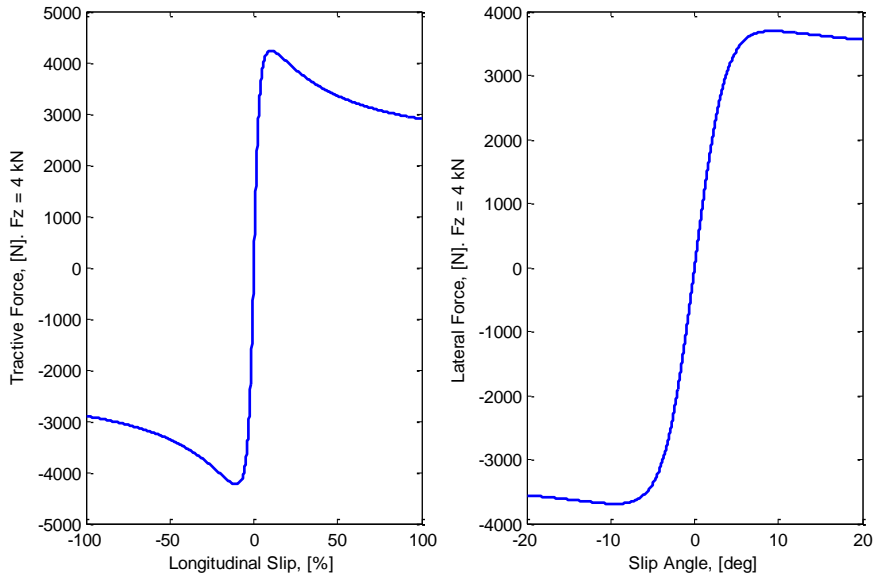


Figure 2.2 A typical tire longitudinal and lateral force profile

When a tire is undergoing combined longitudinal and lateral slip, the available forces remain bounded within an ellipse. Figure 2.3 [Wong, 2001] demonstrates the concept of the friction ellipse. The friction ellipse is used to visualize the maximum available longitudinal and lateral forces in a combined slip condition.
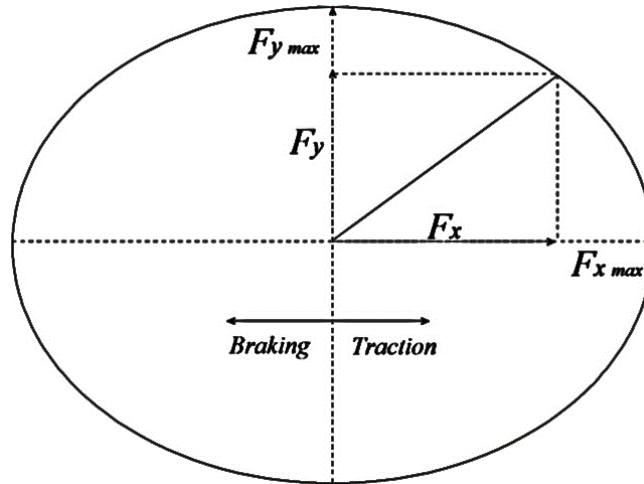
Figure 2.3 The tire friction ellipse

Many different tire models have been developed to predict tire forces in various slip conditions. Tire models can be classified by whether they are derived from first principles modeling or curve fits of empirical data, and whether the tire model describes transient or steady state tire response. A popular first principles steady state model is the Dugoff tire model, also referred to as the HSRI tire model [Svendenius, 2007]. The Dugoff tire model accurately captures tire longitudinal and lateral behavior in low slip conditions, but does not adequately describe the combined slip condition as longitudinal slip and slip angles increase [Wang, 2007]. The Dugoff model is only dependent on 2 parameters, which makes it attractive due to its simplicity, but also limits its predictive capabilities. The LuGre model, developed in [Canudas & Tsiotras, 1999] and [Canudas, et al., 2003] is a dynamic friction model that describes the forces generated by two surfaces sliding past each other. The LuGre model is a lumped parameter transient friction model that captures hysteretic effects; stiction; and the diminishing forces generated at high velocities, known as the Stribeck effect [Uil, 2009], [Svendenius, 2007]. A popular semi-empirical, steady state model is the Pacejka Magic Formula. The Pacejka model is discussed in detail in the following section, as it was used as the tire model in this simulation study.

### 2.2.1 The Pacejka Tire Model

The Pacejka model is based on empirical data, and has been shown to accurately model tire forces for a range of operating conditions at steady state. It is chosen for its accuracy and ease of implementation. In the case of pure slip or pure rolling conditions, the Pacejka Model is given by the following equations [Pacejka, et al., 1987]

$$y(x) = D \sin\left[C \operatorname{atan}\left\{B\, x_{ij} - E\left(B\, x_{ij} - \operatorname{atan}\left(B\, x_{ij}\right)\right)\right\}\right] \tag{2.18}$$

$$x = X + S_h \tag{2.19}$$

$$Y(X) = y(x) + S_v \tag{2.20}$$

where $Y$ is either the lateral tire force with $X_{ij}$ the tire slip angle, or the longitudinal force with $X_{ij}$ the longitudinal wheel slip. The terms $B$, $C$, $D$, and $E$ are experimentally determined coefficients. $B$ represents the stiffness factor, $C$ represents the shape factor, $D$ is the peak factor, and $E$ is the curvature factor. $S_v$ and $S_h$ are vertical and horizontal shifts that allow the model to account for cases when the tire profile is not centered about the origin. These factors can be found as a function of the normal load on a given tire [Wong, 2001].

$$D = a_1 + F_z^2 + a_2 Fz \tag{2.21}$$

$$E = a_6 F_z^2 + a_7 F_z + a_8 \tag{2.22}$$

The product $BCD$ is the slope of the force curve in the linear region. For cornering stiffness, $BCD$ is given by

$$BCD = a_3 \sin[a_4 \tan^{-1}(a_5 F_z)] \tag{2.23}$$

For longitudinal stiffness, the product $BCD$ is given by

$$BCD = \frac{a_3 F_z^2 + a_4 F_z}{e^{a_5 F_z}} \tag{2.24}$$

The shape factor, *C,* is found to be roughly constant regardless of normal load. Its value is 1.30 for determining lateral forces and 1.65 for longitudinal forces. The value of *B* can be found by dividing the previously found products *BCD* and *CD*. The influence of each of these factors can be seen below in Figure 2.4 [Pacejka & Besselink, 1997].
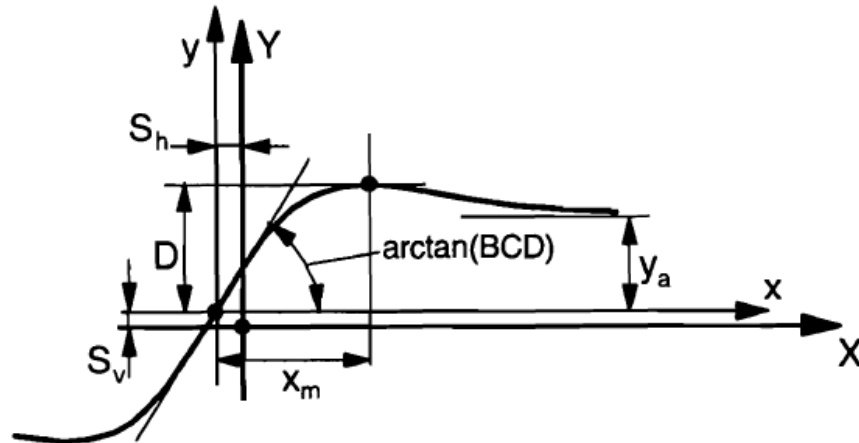


Figure 2.4 Magic Formula coefficients demonstrated on a lateral force curve

The lateral and longitudinal force profiles are shown below for a given set of tire parameters provided in [Wong, 2001].
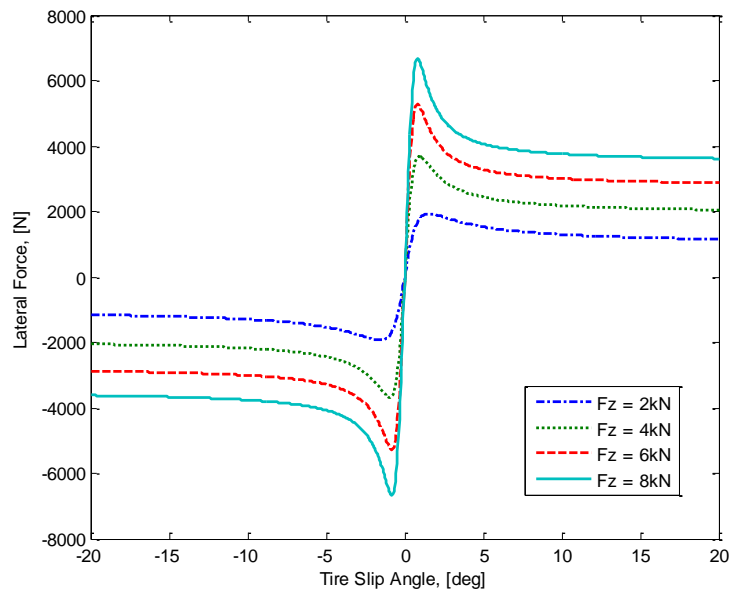


Figure 2.5 Tire lateral force for varying normal load
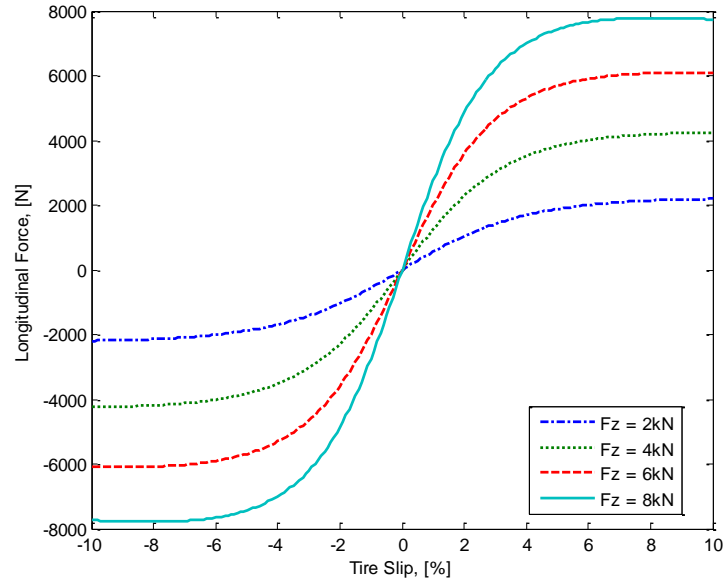
Figure 2.6 Tire longitudinal force for varying normal load

When a tire is undergoing simultaneous braking and turning, the above equations are inadequate [Wong, 2001], [Pacejka & Besselink, 1997]. In the combined lateral and longitudinal slip case, the forces are modified by a weighting function

$$F_* = F_0 G(x) \tag{2.25}$$

$$G(x) = D\,'\cos(C' \tan^{-1}(B'x)) \tag{2.26}$$

Where $x$ is the longitudinal slip when $F_0$ is the lateral force, and $x$ is lateral slip when $F_0$ is longitudinal force. $F_*$ represents the force in the combined slip condition. The terms $B'$, $C'$, and $D'$ are experimentally determined coefficients.
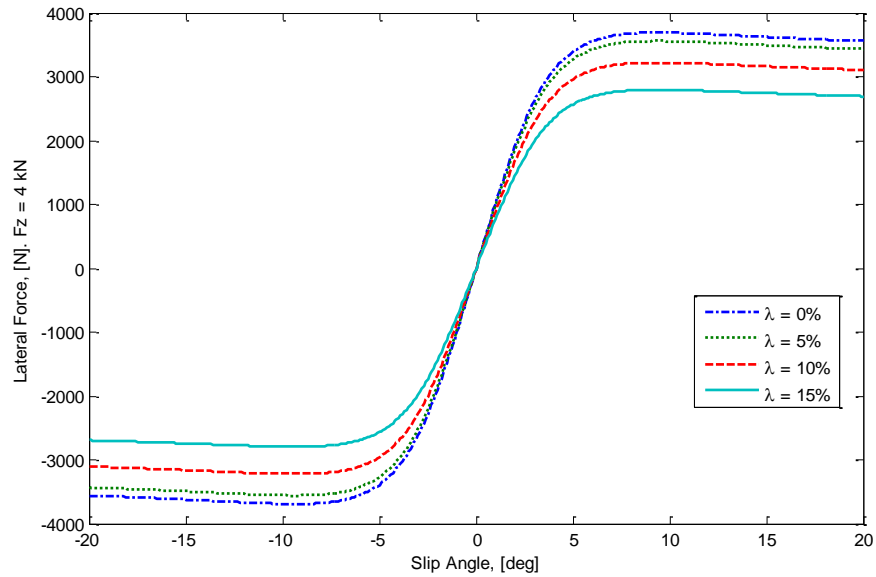
Figure 2.7 Lateral force in the combined slip condition
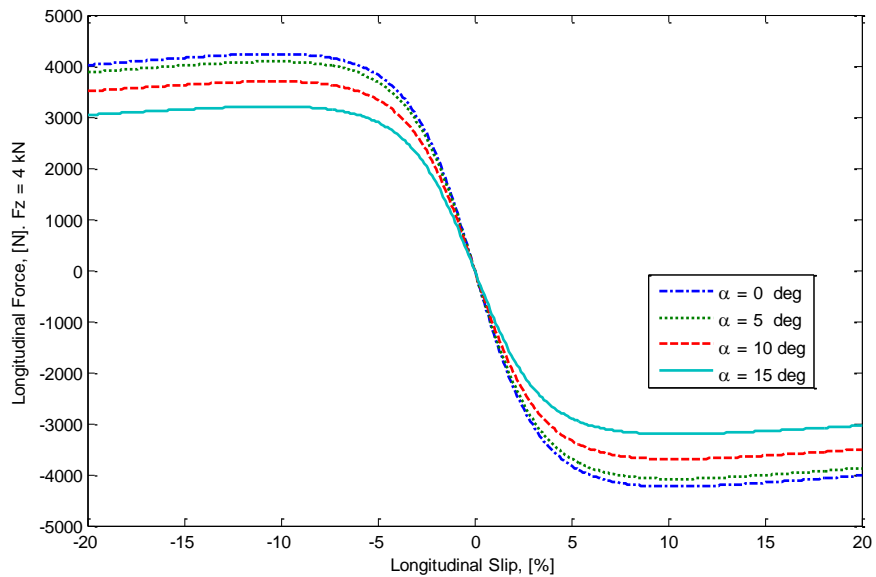


Figure 2.8 Longitudinal force in the combined slip condition

Since the Pacejka coefficients for a given tire are developed using a single road surface, the equations must be modified to account for changing road conditions. A technique known as friction similarity is employed [Wang, 2007]. Begin by defining the friction ratio $R = \mu/\mu_0$, where $\mu$ is the friction coefficient for the current surface and $\mu_0$ is the friction coefficient for the

experimentally determined Pacejka coefficients. Let $\alpha_\mu = \frac{\alpha}{R}$ and $\lambda_\mu = \frac{\lambda}{R}$, where α and λ are the measured slip angle and longitudinal slip, respectively. The updated form of the Magic Formula then becomes

$$y(x_\mu) = RD \sin\left[C \operatorname{atan}\{B\,x_\mu - E(B\,x_\mu - \operatorname{atan}(B\,x_\mu))\}\right] \tag{2.27}$$

$$x_\mu = X_\mu + S_h \tag{2.28}$$

$$Y(X_\mu) = y(x_\mu) + S_v \tag{2.29}$$

Where $X_\mu$ represents $\alpha_\mu$ or $\lambda_\mu$, as appropriate for lateral or longitudinal force calculations. The weighting factor G can also be applied for the case of combined slip.

$$F_{*\mu} = F_{0\mu}G(x_\mu) \tag{2.30}$$

$$G(x_\mu) = D'\cos\left(C'\tan^{-1}(B'x_\mu)\right) \tag{2.31}$$

The effect of varying road conditions is shown for both lateral and longitudinal forces in Figure 2.10 and Figure 2.9.
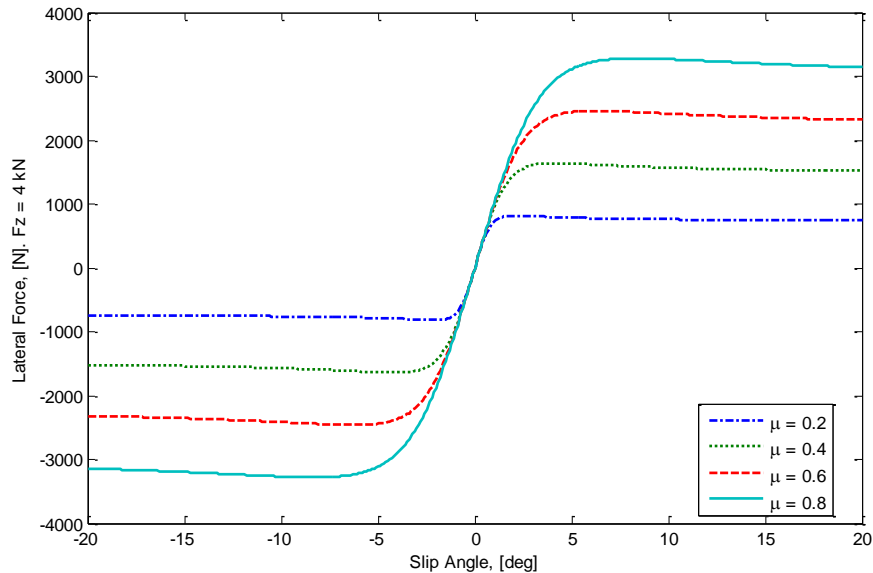


Figure 2.9 Lateral force with varying friction coefficients
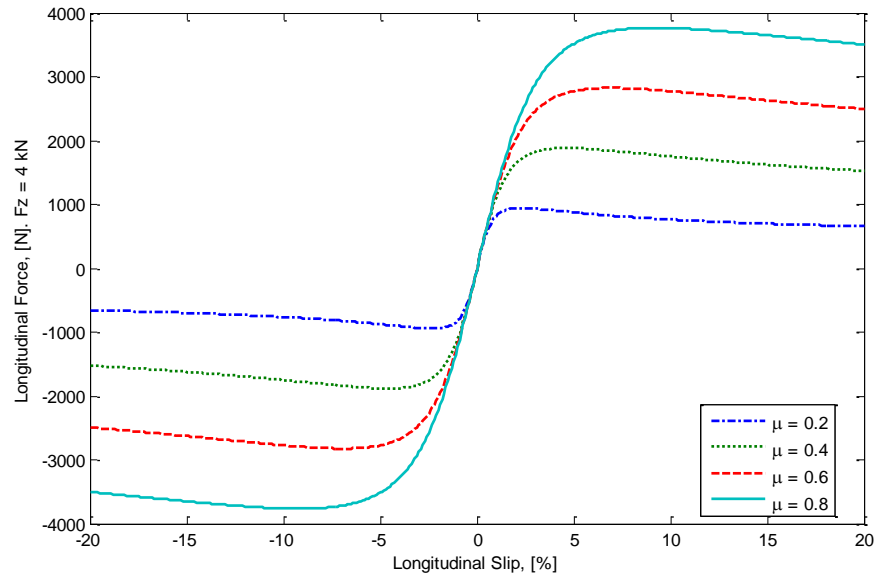
Figure 2.10 Longitudinal force with varying friction coefficients

The most current form of the Pacejka model includes 85 parameters, and has been extended to include effects of camber, inflation pressure, and dynamic responses up to 8 Hz [Uil, 2009], [Svendenius, 2007].

### 2.3 SIMPLIFIED LINEAR MODEL FOR CONTROL

To make controller analysis more tractable, a linearized model is developed. The model is based on the bicycle vehicle model, which makes several assumptions.

- Side slip and steering angles are small
- Dynamic load transfer is negligible
- The tire properties and slip angles are mirrored about the longitudinal axis
- The tire forces are within the linear region

The bicycle model is shown below in Figure 2.11 [Ohara Murakami, 2008].
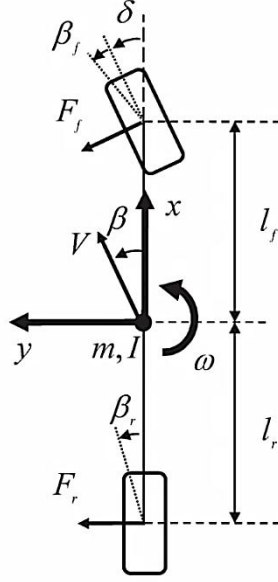
Figure 2.11 Bicycle model

For dynamics linearized about the origin, the equations of motion are given by

$$\dot{V}_x = \frac{1}{m}(F_{xrl} + F_{xrr})$$ ( 2.32 )

$$\dot{V}_y = \frac{1}{m}(F_{yrl} + F_{yrr} + F_{yfl} + F_{yfr})$$ ( 2.33 )

$$\dot{\Omega}_z = \frac{1}{I_z}\left(L_f(F_{yfl} + F_{yfr}) - L_r(F_{yrl} + F_{yrr}) + M\right)$$ ( 2.34 )

$$M = \frac{b_r}{2}(F_{xrr} - F_{xrl})$$ ( 2.35 )

where *M* is treated as a control input for the direct yaw moment controller. Given the linear tire force assumptions and assuming constant longitudinal velocity *V*,

$$F_{yfl} = F_{yfr} = C_f \beta_f = C_f\left(-\beta - \frac{L_f\Omega_z}{V} + \delta_f\right)$$ ( 2.36 )

$$F_{yrl} = F_{yrr} = C_r \beta_r = C_r\left(-\beta + \frac{L_r\Omega_z}{V} + \delta_r\right)$$ ( 2.37 )

$$\dot{V}_y = (\dot{\beta} + \Omega_z)$$ ( 2.38 )

18

Assuming that the rear wheels are unsteered and combining equations yields

$$mV\dot{\beta} + 2(C_f + C_r)\beta + \left[mV + \frac{2}{V}(L_f C_f - L_r C_r)\right]\Omega = 2C_f\delta \qquad (2.39)$$

$$I_z\dot{\Omega} + 2(L_f C_f - L_r C_r)\beta + \frac{2(L_f^2 C_f + L_r^2 C_r)}{V}\Omega = 2L_f C_f\delta + M \qquad (2.40)$$

Which results in the state space formulation

$$\begin{bmatrix} \dot{\beta} \\ \dot{\Omega}_z \end{bmatrix} = \begin{bmatrix} -\dfrac{2(C_f + C_r)}{mV} & -\dfrac{2(C_f L_f - C_r L_r)}{mV^2} - 1 \\ -\dfrac{2(C_f L_f - C_r L_r)}{I_z} & -\dfrac{2(C_f L_f^2 + C_r L_r^2)}{I_z V} \end{bmatrix} \begin{bmatrix} \beta \\ \Omega_z \end{bmatrix} + \begin{bmatrix} \dfrac{2C_f}{mV} & 0 \\ \dfrac{2C_f L_f}{I_z} & \dfrac{1}{I_z} \end{bmatrix} \begin{bmatrix} \delta_f \\ M \end{bmatrix} \qquad (2.41)$$

For the 4WS case, the rear wheel steering angle is taken as a controller input and the yaw moment M is set to zero, resulting in the following state space formulation.

$$\begin{bmatrix} \dot{\beta} \\ \dot{\Omega}_z \end{bmatrix} = \begin{bmatrix} -\dfrac{2(C_f + C_r)}{mV} & -\dfrac{2(C_f L_f - C_r L_r)}{mV^2} - 1 \\ -\dfrac{2(C_f L_f - C_r L_r)}{I_z} & -\dfrac{2(C_f L_f^2 + C_r L_r^2)}{I_z V} \end{bmatrix} \begin{bmatrix} \beta \\ \Omega_z \end{bmatrix} + \begin{bmatrix} \dfrac{2C_f}{mV} & \dfrac{2C_r}{mV} \\ \dfrac{2C_f L_f}{I_z} & -\dfrac{2L_r Cr}{I_z} \end{bmatrix} \begin{bmatrix} \delta_f \\ \delta_r \end{bmatrix} \qquad (2.42)$$

Figure 2.12 below compares the linear and nonlinear system response to a low speed double lane change on a high friction road. The responses are nearly identical, demonstrating the validity of the linearized model during typical driving conditions.
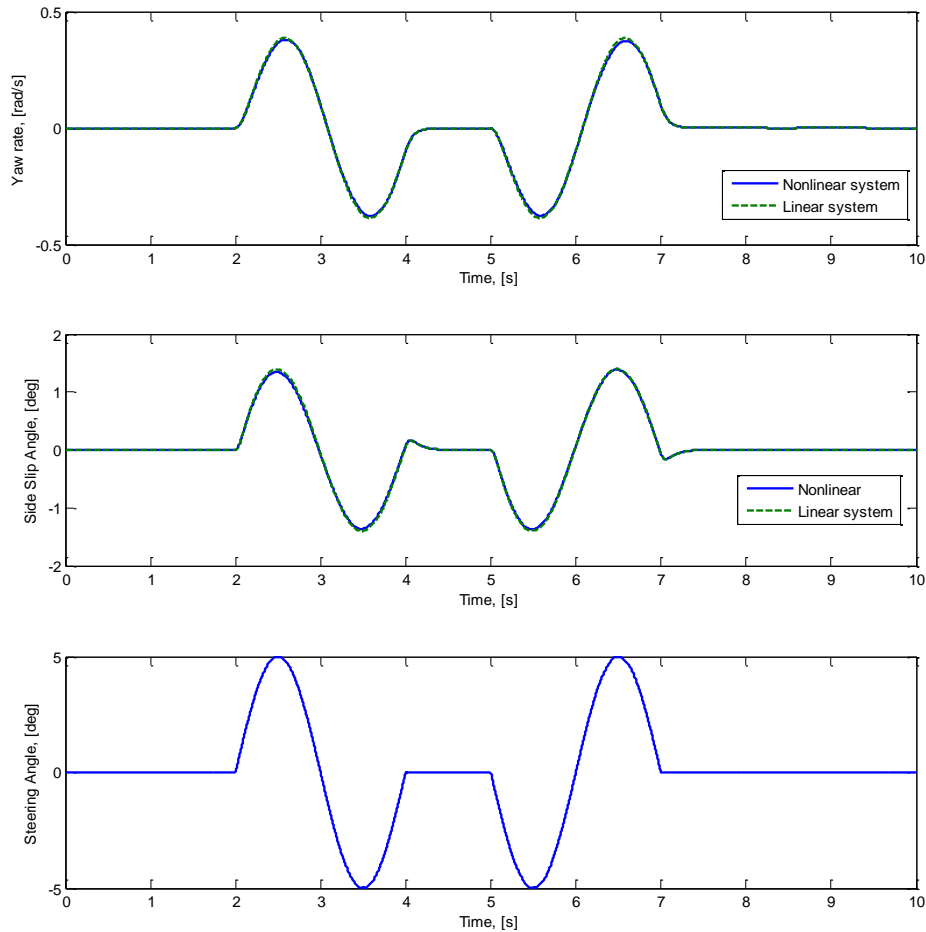
Figure 2.12 Comparison of linear and nonlinear system response to a 50 km/h double lane change

### 2.3.1 Rocard Stability Analysis

The Rocard stability analysis was one of the first techniques used to determine the directional stability of a simplified, linear vehicle model. Directional stability refers to the behavior of a vehicle in the presence of an external disturbance force or moment. A directionally stable vehicle, when disturbed, will only vary slightly from its original trajectory, whereas a directionally unstable vehicle will follow a path that increasingly deviates from the original.

An abbreviated derivation of the stability criterion is presented here [Steeds, 1960]. The following differential equations are derived for the angular and lateral velocity of the vehicle.

$$M\ddot{y} + 2\left(\frac{C_f + C_r}{V_x}\right)\dot{y} + 2\left(\frac{L_f C_f - L_r C_r}{V_x}\right)\dot{\theta} - 2(C_f + C_r)\theta = F \qquad (2.43)$$

$$I_z\ddot{\theta} + \frac{2(C_f L_f - C_r L_r)}{V_x}\dot{y} + \frac{2(C_f L_f^2 + C_r L_r^2)}{V_x}\dot{\theta} - 2(C_f L_r - C_r L_r)\theta = C \qquad (2.44)$$

where $C_f$ and $C_r$ are the front and rear cornering stiffness, $L_f$ and $L_r$ are the distance to the front and rear axle from the c.g., $\Theta$ is the vehicle angle, $F$ represents any external forces, and $C$ represents any external moments. The ODEs are rewritten in terms of $\psi = \frac{y}{k}$, a dimensionless quantity where k is the radius of gyration and $I_z=Mk^2$.

$$\frac{dy}{dt} = \frac{kd\psi}{dt} \qquad (2.45)$$

$$\frac{d^2y}{dt^2} = \frac{kd^2\psi}{dt^2} \qquad (2.46)$$

Equations ( 2.45 ) and ( 2.46 ) are substituted in to equations ( 2.43 ) and ( 2.44 ) and normalized by *Mk* and *Mk²* to give

$$\ddot{\psi} + 2\left(\frac{C_f + C_r}{MV_x}\right)\dot{\psi} + 2\left(\frac{L_f C_f - L_r C_r}{MkV_x}\right)\dot{\theta} - \frac{2(C_f + C_r)}{Mk}\theta = \frac{F}{Mk} \qquad (2.47)$$

$$\ddot{\theta} + \frac{2(C_f L_f - C_r L_r)}{MkV_x}\dot{y} + \frac{2(C_f L_f^2 + C_r L_r^2)}{Mk^2 V_x}\dot{\theta} - \frac{2(C_f L_r - C_r L_r)}{Mk^2}\theta = \frac{C}{Mk^2} \qquad (2.48)$$

By assuming that the solution takes the form $\psi = e^{\lambda t}$ and $\Theta = e^{\lambda t}$ for *F=C=0*, the equations can be written as

$$\left[\lambda^2 + \frac{2\lambda(C_f + C_r)}{MV_x}\right]\psi + \left[\frac{2\lambda(L_f C_f - L_r C_r)}{MkV_x} - \frac{2(C_f + Cr)}{Mk}\right]\theta = 0 \qquad (2.49)$$

$$\left[\frac{2(L_f C_f - L_r C_r)}{MkV_x}\lambda\right]\psi + \left[\lambda^2 + \frac{2\lambda(C_f L_f^2 + C_r L_r^2)}{Mk^2 V_x} - \frac{2(C_f L_f - C_r L_r)}{Mk^2}\right]\theta = 0 \qquad (2.50)$$

After some algebraic manipulation, the equations are finally written as

21

$$\lambda^2 + R\lambda + S = 0 \tag{2.51}$$

$$R = \frac{2}{mV_x}\left[C_f\left(1 + \frac{L_f^2}{k^2}\right) + C_r\left(1 + \frac{L_2^2}{k^2}\right)\right] \tag{2.52}$$

$$S = \frac{4C_f C_r\left(L_f + L_r\right)^2}{m^2 k^2 V_x^2} - \frac{2\left(C_f L_f - C_r L_r\right)}{mk^2} \tag{2.53}$$

For a stable linear system, the eigenvalues must be negative, and therefore both $R$ and $S$ must be positive. Since $R$ is clearly always positive, a condition is placed on $S$ such that the first term is greater than the second. This can be solved in terms of a critical velocity $V_c^2$ as follows

$$V_c^2 = \frac{2C_f C_r\left(L_f + L_r\right)^2}{m(C_f L_f - C_r L_r)} \tag{2.54}$$

Thus, a critical velocity exists if

$$C_f L_1 > C_r L_2 \tag{2.55}$$

Below this critical velocity, the system is always directionally stable.

The Rocard analysis ties closely with the modern concepts of oversteer, neutral steer, and understeer. The understeer coefficient, $K_{us}$ is defined as

$$K_{us} = \frac{W_f}{C_f} - \frac{W_r}{C_r} \tag{2.56}$$

where $W_f$ and $Wr$ is the weight of the vehicle on the front and rear tires, respectively [Wong, 2001]. It can be seen by inspection that the understeer condition is simply a restatement of the stability criteria of equation ( 2.55 ). The understeer coefficient is used to calculate the steering angle required to negotiate a constant radius turn of radius $R$.

$$\delta_f = \frac{L}{R} + \frac{V^2}{gR}K_{us} \tag{2.57}$$

In a vehicle with neutral steer, $K_{us}=0$, and the steering angle required for a given turn is independent of the forward velocity. In oversteer, $K_{us} < 0$, indicating that the required steering input decreases with increasing velocity. In understeer, $K_{us} > 0$, and the required steering input increases with increasing velocity. These relationships are demonstrated below in Figure 2.13.
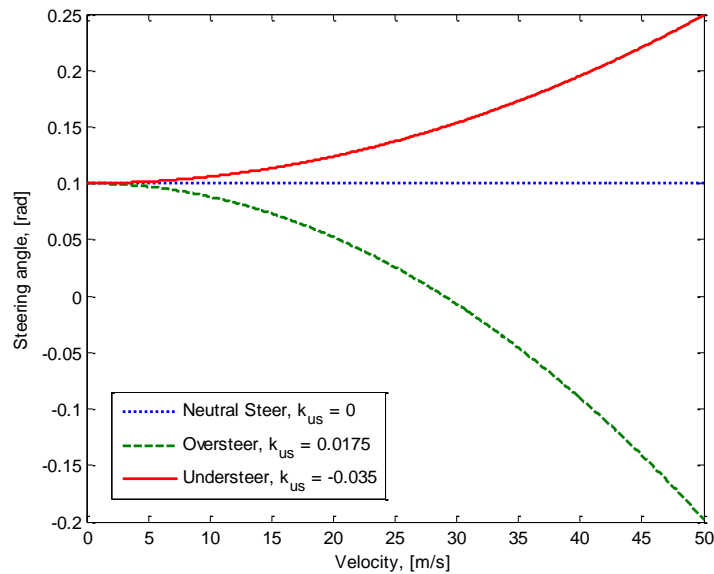


Figure 2.13 Effect of understeer coefficient on required steering angle

For a vehicle in oversteer, the system is unstable above a particular critical velocity at which the required angle to negotiate a given turn is 0. The critical velocity can be expressed in terms of the understeer coefficient as

$$V_{crit} = \sqrt{\frac{gL}{-K_{us}}}$$

( 2.58 )

**2.4 REFERENCE MODEL DEVELOPMENT**

Following the development presented in [Shino & Nagai, 2001] and [Mirzaei, 2010], the yaw rate response of the linear bicycle model is represented in transfer function form.

$$\frac{\Omega(s)}{\delta(s)} = \frac{G_\Omega(1 + T_\Omega s)}{1 - \frac{T_A}{D_A}s + \frac{1}{D_A}s^2} \qquad (2.59)$$

Where

$$G_\Omega = \frac{b_1 a_{21} - b_2 a_{11}}{D_A} \qquad (2.60)$$

$$T_\Omega = \frac{b_2}{b_1 a_{21} - b_2 a_{11}} \qquad (2.61)$$

$$T_A = a_{11} + a_{22} \qquad (2.62)$$

$$D_A = a_{11}a_{22} - a_{12}a_{21} \qquad (2.63)$$

and the terms $a_{ij}$ and $b_i$ refer to their corresponding matrix elements in the state space representation of the bicycle model, shown here for convenience.

$$\begin{bmatrix} \dot{\beta} \\ \dot{\Omega}_z \end{bmatrix} = \begin{bmatrix} -\frac{2(C_f + C_r)}{mV} & -\frac{2(C_f L_f - C_r L_r)}{mV^2} - 1 \\ -\frac{2(C_f L_f - C_r L_r)}{I_z} & -\frac{2(C_f L_f^2 + C_r L_r^2)}{I_z V} \end{bmatrix} \begin{bmatrix} \beta \\ \Omega_z \end{bmatrix} + \begin{bmatrix} \frac{2C_f}{mV} \\ \frac{2C_f L_f}{I_z} \end{bmatrix} \delta_f \qquad (2.64)$$

As originally proposed in [Mokhiamar & Abe, 2002b], the reference vehicle yaw rate response is simplified to a first order lag. The desired side slip angle is set to zero, and the reference yaw rate then becomes

$$\frac{\Omega(s)}{\delta(s)} = \frac{G_\Omega}{1 + T_\Omega s} \qquad (2.65)$$

A reference model of this type is common in vehicle handling research, and has been used in [Shino & Nagai, 2001], [Ohara & Murakami, 2008], and [Jianyong, et al., 2007]. [Mirzaei, 2010] treats the desired side slip angle as a first order lag and uses the same first order response for the desired yaw rate. An alternative approach is to use a driver model in the yaw rate reference. [Wang & Hsieh, 2009] use a driver steering model to generate the desired yaw

rate, and [Mokhiamar & Abe, 2002a] use a path planning algorithm to determine the appropriate reference yaw rate to track a desired trajectory.

# Chapter 3: Design of Controller

A brief background on control theory is presented, and relevant definitions, properties, and theorems are established. The MRAC controller is then developed, and proof of convergence is shown for the adaptive and non-adaptive cases. The requisite properties of the system state and input matrices are established, and it is shown that the present technique for adaptive control is not implementable for a 4WS controller. For completeness, a discussion of tire slip controllers is presented, and a simple tire slip controller is developed.

## 3.1 CONTROL THEORY BACKGROUND

Before discussing stability of the dynamic system, some terms and properties of functions must be defined.

**Definition 3.1: LP Spaces** Consider any function $f: \mathcal{R} \to \mathcal{R}^n$. The P norm is defined as $\|f\|_p = \left[\int_{-\infty}^{\infty} |f(\sigma)|^p d\sigma\right]^{\frac{1}{p}}$ for any positive integer p. Additionally the infinity norm is defined as $\|f\|_\infty = \sup(|f(t)|)$. Any function $f$ is said to belong to L$_P$ if $\|f\|_p$ is finite.

**Definition 3.2: Barbalet's Lemma** For any scalar valued function with real inputs and real outputs, if $\lim\limits_{t \to \infty} \int_0^t f(\sigma)d\sigma$ exists and is finite, and f(t) is uniformly continuous, then $\lim\limits_{t \to \infty} f(t) = 0$. A sufficient condition for a function to be considered uniformly continuous is that $\dot{f}(t) \in L_\infty$. As a corollary to Barbalet's lemma, consider the real, scalar valued function $f(t)$. If $f \in L_p \cap L_\infty$ for some positive integer P, and $\dot{f} \in L_\infty$, then $\lim\limits_{t \to \infty} f(t) = 0$.

**Definition 3.3: Class K, KR Functions** A class K function is any continuous, scalar valued function $\psi: [0, r] \to \mathcal{R}^+$ where $\psi$ satisfies the conditions *ψ(0) = 0* and $\psi$ is strictly increasing on [0,r]. A class KR function is defined as a class K function where $r = \infty$ and $\lim\limits_{t \to \infty} \psi(t) = \infty$.

**Definition 3.4: Positive Definite** A function $V(t, x): \mathcal{R}^+ \times B_r(0) \to \mathcal{R}$ with $V(t, 0) = 0 \ \forall \ t \in \mathcal{R}^+$ is positive definite on $x \in B_r(0) \subset \mathcal{R}^n$ if there exists a class K function $\psi$ such that $V(t, x) \geq \psi(|x|)$ for $t \geq 0$ and $x \in B_r(0) \subset \mathcal{R}^n$ for some $r > 0$. A weaker condition is positive semi-definite, which requires that $V(t, x) \geq 0$ for $t \geq 0$ and $x \in B_r(0) \subset \mathcal{R}^n$ for some $r > 0$.

**Definition 3.5: Radially Unbounded** A function $V(t,x): \mathcal{R}^+ \times B_r(0) \to \mathcal{R}$ with $V(t,0) = 0 \; \forall \; t \in \mathcal{R}^+$ is radially unbounded on $x \in B_r(0) \subset \mathcal{R}^n$ if there exists a class KR function $\psi$ such that $V(t,x) \geq \psi(|x|)$ for $t \geq 0$ and $x \in B_r(0) \subset \mathcal{R}^n$ for some $r > 0$.

**Definition 3.6: Decrescent** A function $V(t,x): \mathcal{R}^+ \times B_r(0) \to \mathcal{R}$ with $V(t,0) = 0 \; \forall \; t \in \mathcal{R}^+$ is decrescent on $x \in B_r(0) \subset \mathcal{R}^n$ if there exists a class KR function $\psi$ such that $V(t,x) \leq \psi(|x|)$ for $t \geq 0$ and $x \in B_r(0) \subset \mathcal{R}^n$ for some $r > 0$.

In addition to the above definitions, certain properties of the trace must be established. The trace operator has three important properties that will be used in the controller derivation [Ioannou & Sun, 2012].

1. $tr(AB) = tr(BA)$
2. $tr(A + B) = tr(A) + tr(B)$ for any $A, B \in \mathcal{R}^{nxn}$
3. $tr(yx^T) = x^T y$ for any $x, y \in \mathcal{R}^{nx1}$

### 3.1.1 Lyapunov Stability Analysis

Lyapunov analysis provides a sufficient, but not necessary condition on system stability. A brief background is provided on different classifications of stability and the requirements for each [Ioannou & Sun, 2012].

To begin, consider the system $\dot{x} = f(t,x)$ with $t \geq 0$ and $x \in B_r(0) \subset \mathcal{R}^n$ with the equilibrium point $x = x_e$ where $f(t, x_e) = 0$. For the sake of simplicity, the system is taken to be time invariant such that $\dot{x} = f(x)$.

**Definition 3.7: Stable** The equilibrium point $x_e$ is said to be stable if for any given $t_0$ and $\epsilon > 0$, there exists some $\delta(t_0,\epsilon)$ such that $\|x_0 - x_e\| < \delta$ implies that $\|x(t) - x_e\| < \epsilon$ for all $t \geq t_0$. That is to say, once $x_0$ is within some initial distance $\delta$ of the equilibrium point, it will remain within a distance $\epsilon$ for all time after.

**Definition 3.8: Uniformly Stable** An equilibrium point is considered to be uniformly stable if the value of $\delta$ from above is independent of the initial time $t_0$.

**Definition 3.9: Asymptotically Stable** An equilibrium point is asymptotically stable if there exists some $\delta(t_0)$ such that $\|x_0 - x_e\| < \delta$ implies that $\lim_{t \to \infty} \|x(t) - x_e\| = 0$. For an asymptotically stable equilibrium point, the system will converge to $x_e$ once it is within some distance $\delta$.

**Definition 3.10: Uniformly Asymptotically Stable** An equilibrium point is considered to be uniformly asymptotically stable if the value of $\delta$ from above is independent of the initial time $t_0$.

**Definition 3.11: Exponentially Stable** An equilibrium point is exponentially stable if there exists some $\alpha > 0$ and for all $\epsilon > 0$ there exists $\delta(\epsilon)$ such that $\|x(t) - x_e\| \leq ke^{-\alpha(t-t_0)}$ whenever $\|x_0 - x_e\| < \delta$.

With the above definitions established, the theorem of Lyapunov can now be presented.

**Theorem of Lyapunov** Consider again the system $\dot{x} = f(x)$ with $t \geq 0$ and $x \in B_r(0) \subset \mathcal{R}^n$ with the equilibrium point $x_e = 0$. Given a function $V(t,x) : \mathcal{R}^+ \times B_r(0) \to \mathcal{R}$ with $V(t,0) = 0 \; \forall \; t \in \mathcal{R}^+$ for some $r > 0$ and $B_r(0) \subset \mathcal{R}^n$ such that $\frac{\partial V}{\partial x}$ are defined, the following conditions hold true.

**Condition 1**: If $\dot{V}(t,x) \triangleq \frac{\partial V}{\partial x}$ is negative semi-definite, then $x_e$ is stable in the sense of Lyapunov (ISL).

**Condition 2**: If in addition to condition 1, V is decrescent, then $x_e$ is uniformly stable ISL.

**Condition 3**: If $\dot{V}(x)$ is negative definite and V is decrescent, $x_e$ is uniform asymptotically stable.

**Condition 4**: If V is decrescent and there exist class K functions $\psi_1$, $\psi_2$, and $\psi_3$ with the same order of magnitude such that $\psi_1(|x|) \leq V(t,x) \leq \psi_2(|x|)$ and $\dot{V}(x) \leq -\psi_3(|x|)$, then $x_e$ is exponentially stable.

### 3.1.2  Adaptive Control Background

The goal of adaptive control is to derive a control law that guarantees asymptotic convergence of tracking error and is independent of unknown system parameters. Estimates of the parameters are used, and an update scheme is developed to generate better estimates of

the unknown parameters as the system operates. Typically, the adaptive parameter estimates will not converge to the true values of the parameters. An additional requirement of the controller is that all states, control inputs, and parameter estimates remain bounded during operation. An illustrative example is presented for a single input, single output (SISO) system.

Consider the nonlinear pendulum shown below in Figure 3.
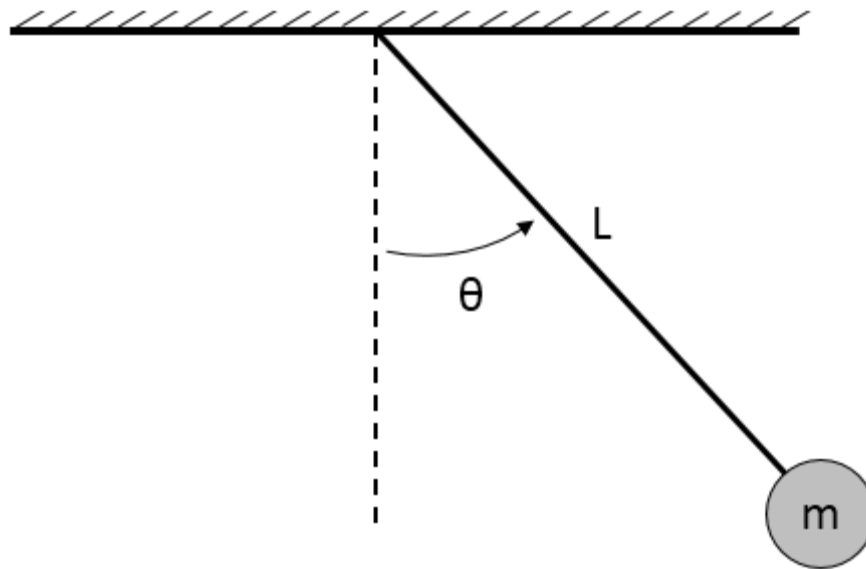


Figure 3.14 A nonlinear pendulum

The system dynamics are given by

$$\begin{bmatrix} \dot{\theta}_1 \\ \dot{\theta}_2 \end{bmatrix} = \begin{bmatrix} \theta_2 \\ -\frac{g}{L}\sin(\theta_1) + u \end{bmatrix} \qquad (3.1)$$

where $\vartheta_1$ represents the angular position, $\vartheta_2$ is the angular velocity, $g$ is the acceleration due to gravity, and $L$ is an unknown constant representing length. The control input $u$ is a torque exerted about the pivot point. For simplicity, let $A^*$ represent the unknown constant $-\frac{g}{L}$. The goal of the system is to track the reference position $\vartheta_r$, which is given by

29

$$\theta_r = \frac{\pi}{4} + \frac{\pi}{12}\sin(\pi t) \tag{3.2}$$

The tracking error is given by

$$\begin{bmatrix} e_1 \\ e_2 \end{bmatrix} = \begin{bmatrix} \theta_1 - \theta_r \\ \theta_2 - \dot{\theta}_r \end{bmatrix} \tag{3.3}$$

The tracking error dynamics are then

$$\begin{bmatrix} \dot{e}_1 \\ \dot{e}_2 \end{bmatrix} = \begin{bmatrix} e_2 \\ A^* \sin(\theta_1) + u - \ddot{\theta}_r \end{bmatrix} \tag{3.4}$$

It is assumed that all states are available for feedback, and it can be shown that the system is controllable. In the known case, the control law would be chosen as

$$u = -A^* \sin(\theta_1) + \ddot{\theta}_r - \alpha e_2 - (e_2 + \alpha e_1) \tag{3.5}$$

Where α is a positive constant. A Lyapunov candidate is selected as

$$V = \frac{1}{2}(e_2 + \alpha e_1)^2 \tag{3.6}$$

Taking the derivative of V and replacing the derivatives of error with their respective dynamics yields

$$\dot{V} = -(e_2 + \alpha e_1)^2 \tag{3.7}$$

When the system parameters are unknown, an estimate for $A^*$ must be used instead. The parameter estimation error is defined as

$$\tilde{A} = \hat{A} - A^* \tag{3.8}$$

Where $\hat{A}$ is defined as the parameter estimate. The control law then becomes

$$u = -\hat{A}\sin(\theta_1) + \ddot{\theta}_r - \alpha e_2 - (e_2 + \alpha e_1) \tag{3.9}$$

A new Lyapunov candidate is proposed that includes the tracking error and the parameter estimate

$$V = \frac{1}{2}(e_2 + \alpha e_1)^2 + \frac{1}{2\gamma}\tilde{A}^2 \qquad (3.10)$$

The term $\gamma$ is a positive constant that acts as the adaptive update rate. As in the known parameter case, the derivative of the Lyapunov candidate is solved for and the error dynamics are substituted for their respective error derivatives. After simplification, the derivative of the Lyapunov candidate becomes

$$\dot{V} = -(e_2 + \alpha e_1)^2 + \tilde{A}\left[\frac{1}{\gamma}\dot{\hat{A}} - (e_2 + \alpha e_1)\sin(\theta_1)\right] \qquad (3.11)$$

Finally, the adaptive update law is chosen to cancel the undesired terms.

$$\dot{\hat{A}} = \gamma(e_2 + \alpha e_1)\sin(\theta_1) \qquad (3.12)$$

Standard signal chasing arguments can be employed to prove the boundedness of all control signals, system states, and parameter estimates, as well as asymptotic convergence of the tracking error. A proof of this type will be presented for the MIMO adaptive controller developed in the following section. The system is simulated for 15 seconds given initial tracking and parameter estimate errors. As expected, the system achieves asymptotic tracking with bounded parameter estimates and controller inputs. In this case the parameter estimate does converge to the actual value, however, this is not guaranteed to occur.

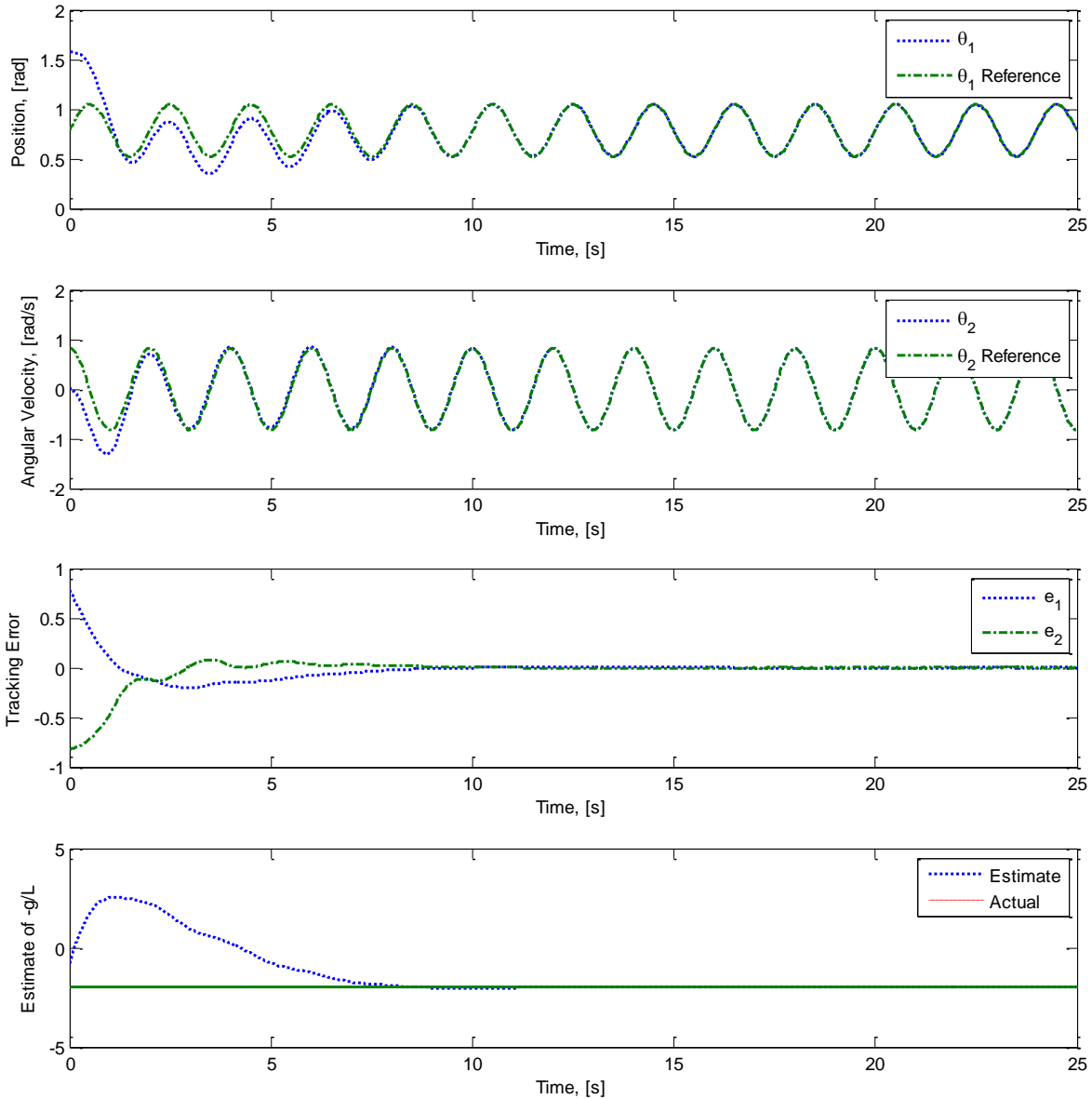Figure 3.15 Pendulum tracking performance with adaptive control

The SISO example from above can be modified to work on MIMO systems if the input matrix *B* is square and invertible. Additionally, the control law can be configured for both unknown input and state matrices so long as certain properties of the input matrix can be established. An adaptive controller of this type is developed in section 3.2.

### 3.1.3 Complications in Adaptive Control

Though adaptive control can improve performance in cases where the initial parameter estimates are incorrect, it is not without its downsides. The first problem that can arise in the development of an adaptive controller is the uniform detectability obstacle. As an example, consider stabilization of the following linear system

$$\begin{bmatrix} \dot{x}_1 \\ \dot{x}_2 \end{bmatrix} = \begin{bmatrix} x_2 \\ a_1 x_1 + a_2 x_2 + u \end{bmatrix} \qquad (3.13)$$

Where $a_1$ and $a_2$ are unknown constants and u is the controller input. In the case of known parameters, the control input would be

$$u = -a_1 x_1 - a_2 x_2 - k_1 x_1 - k_2 x_2 \qquad (3.14)$$

For any positive constants $k_1$ and $k_2$. It is easily shown that this control law leads to asymptotic convergence to the origin. In the adaptive control case, the unknown parameters are replaced with estimates as previously done in equation ( 3.8 ). The closed loop dynamics then become

$$\begin{bmatrix} \dot{x}_1 \\ \dot{x}_2 \end{bmatrix} = \begin{bmatrix} x_2 \\ -\hat{a}_1 x_1 - \hat{a}_2 x_2 - k_1 x_1 - k_2 x_2 \end{bmatrix} \qquad (3.15)$$

A Lyapunov candidate function is chosen that includes the system states and parameter estimation errors.

$$V = \frac{1}{2}\tilde{a}_1^2 + \frac{1}{2}\tilde{a}_2^2 + \frac{k_1}{2}x_1^2 + \frac{k_2}{2}x_2^2 \qquad (3.16)$$

$$\dot{V} = -k_2 x_2^2 - \tilde{a}_1 x_1 x_2 - \tilde{a}_2 x_2^2 + \tilde{a}_1 \dot{\hat{a}}_1 + \tilde{a}_2 \dot{\hat{a}}_2 \qquad (3.17)$$

The parameter update terms are selected to cancel out the terms of non-definite sign

$$\dot{\hat{a}}_1 = x_1 x_2 \qquad (3.18)$$

$$\dot{\hat{a}}_2 = x_2^2 \tag{3.19}$$

Which leaves $\dot{V} = -k_2 x_2^2 \leq 0$. Since V is lower bounded and decreasing, $V \in L_\infty$, which gives $x_1, x_2, \tilde{a}_1, \tilde{a}_2 \in L_\infty$. Additionally, $\lim_{t\to\infty} V(t) = V_\infty$ exists and is finite. Since $\lim_{t\to\infty} \int_0^t \dot{V}(\tau)d\tau = \lim_{t\to\infty} \int_0^t -k_2 x_2^2 \, d\tau = V(0) - V_\infty \Rightarrow x_2 \in L_2$. All elements composing the control input u are $L_\infty$, therefore $u \in L_\infty$. By the same reasoning, $\dot{x}_2 \in L_\infty$. By Barbalet's lemma, since $x_2 \in L_2 \cap L_\infty$ and $\dot{x}_2 \in L_\infty$, then $\lim_{t\to\infty} x_2(t) = 0$. Simply knowing that $\lim_{t\to\infty} x_2(t) = 0$ and $\dot{x}_1 = x_2$ is not sufficient to claim that $\lim_{t\to\infty} x_1(t) = 0$, or even to claim that the limit exists.

To investigate x₁(t), consider the behavior of $\dot{x}_2$ using Barbalet's lemma. First, $\lim_{t\to\infty} \int_0^t \dot{x}_2(\tau)d\tau = \lim_{t\to\infty}[x_2(t)] - x_2(0) = x_2(0)$, meaning that the integral exists and the solution is a finite constant. Next it is shown that $\dot{x}_2$ is uniformly continuous, since $\ddot{x}_2 \epsilon L_\infty$. Barbalet's lemma guarantees that $\lim_{t\to\infty} \dot{x}_2(t) = 0$. It is also true that $\lim_{t\to\infty} \dot{x}_2(t) = -(k_1 + \tilde{a}_1)x_1$. Unless the sum $-(k_1 + \tilde{a}_1)$ can be prevented from going to 0, the behavior of $\lim_{t\to\infty} x_1(t)$ cannot be guaranteed. The uniform detectability obstacle occurs whenever the derivative of the Lyapunov candidate is non-strict in the known parameter case, and can be avoided by careful selection of Lyapunov candidate.

A second problem faced by adaptive controllers is unbounded parameter estimates in the presence of an external disturbance. It can be shown that even a bounded, time decaying disturbance can cause unbounded parameter estimates [Akella, 2013]. Consider the linear, scalar system

$$\dot{x} = ax + u + d(t) \tag{3.20}$$

Where *a* is an unknown constant and *d(t)* is an unknown, bounded disturbance. First, a controller is derived for stabilization in the case of $d(t) = 0$. For any *a_m>0*, the state equation can be re-written as

$$\dot{x} = -a_m x + (a + a_m)x + u \tag{3.21}$$

If we let $k^* = a + a_m$, then the controller input and adaptive update law can be written as

$$u = -\hat{k}x \qquad (3.22)$$

$$\dot{\hat{k}} = \gamma x^2 \qquad (3.23)$$

where $\gamma$ is any positive constant. This control law and update scheme can be shown to guarantee perfect tracking with bounded controller input and parameter estimates. A bounded disturbance force d(t) is selected to be

$$d(t) = (1+t)^{-\frac{1}{5}}\left[5 - (1+t)^{-\frac{1}{5}} - \frac{2}{5}(1+t)^{-\frac{6}{5}}\right] \qquad (3.24)$$

For this disturbance, the time solution for x(t) and $\hat{k}(t)$ can be expressed as

$$x(t) = (1+t)^{-\frac{2}{5}} \qquad (3.25)$$

$$\hat{k}(t) = 5(1+t)^{\frac{1}{5}} \qquad (3.26)$$

While it is clear that *x(t)* still decays to the origin as intended, the parameter estimate increases without bound. Robustness modifications exist that can guarantee convergence of the tracking error to within a residual set while preventing unbounded parameter drift, however, development of such modifications is left for future work.

## 3.2 DERIVATION OF CONTROLLER AND ADAPTIVE UPDATE LAWS

In this section the controller is developed using the simplified model of section 2.3. The controller development is first shown for the known parameter case, and is then extended to included adaptive parameter estimates. Convergence of the tracking error is shown in section 3.2.3, and requisite properties of the state space matrices are established in section 3.2.4.

### 3.2.1 Controller Derivation for Known Parameter Case

To derive the controller, the linearized 2 DOF system model is used. In general, the state space formulation of the system can be described as

$$\dot{x} = Ax + Bu \qquad (3.27)$$

where x is a vector of the system states ($x \in \mathcal{R}^{nx1}$), A is the state matrix ($A \in \mathcal{R}^{nxn}$), u is the control input ($u \in \mathcal{R}^{mx1}$), and B is the input matrix ($B \in \mathcal{R}^{nxm}$). Let $x_d$ be a bounded reference signal with a bounded derivative ($x_d \in \mathcal{R}^{nx1}$), where

$$x_d = \begin{bmatrix} \beta_d \\ \Omega_d \end{bmatrix} \qquad (3.28)$$

Let the error e and its derivative $\dot{e}$ be defined as

$$e = x - x_d$$
$$\dot{e} = \dot{x} - \dot{x}_d \qquad (3.29)$$

Substituting the system dynamics for $\dot{x}$ yields

$$\dot{e} = Ax + Bu - \dot{x}_d \qquad (3.30)$$

Let $A_m$ be any Hurwitz matrix ($A_m \in \mathcal{R}^{nxn}$). Adding and subtracting $A_m$e to equation ( 3.30 ) and rearranging leaves us with

$$\dot{e} = A_m e + B[u + K^*x - L^*(A_m e + \dot{x}_d)] \qquad (3.31)$$

$K^*$ and $L^*$ ($K^*, L^* \in \mathcal{R}^{mxn}$) are given by the following equations, known as the matching conditions.

$$BK^* = A$$
$$BL^* = I \qquad (3.32)$$

where $I$ is the identity matrix ($I \in \mathcal{R}^{nxn}$). The control input u is selected to drive the error term to zero.

$$u = -K^*x + L^*(A_m e + \dot{x}_d) \qquad (3.33)$$

The error dynamics are then

$$\dot{e} = A_m e \qquad (3.34)$$

Since $A_m$ is Hurwitz, $\lim\limits_{t \to \infty} e(t) = 0$.

### 3.2.2  Derivation of Adaptive Update Laws

In the adaptive case, the matrices $A$ and $B$ contain unknown elements, so $K^*$ and $L^*$ cannot be computed directly. Instead, adaptive estimates of each must be used. Let $\hat{K}$ and $\hat{L}$ be estimates of $K^*$ and $L^*$. The parameter estimation error is given by

$$\tilde{K} = \hat{K} - K^*$$
$$\tilde{L} = \hat{L} - L^* \qquad (3.35)$$

The control law and error dynamics for the unknown parameter case become

$$u = -\hat{K}x + \hat{L}(A_m e + \dot{x}_d) \qquad (3.36)$$
$$\dot{e} = A_m e - B\tilde{K}x + B\tilde{L}(A_m e + \dot{x}_d) \qquad (3.37)$$

Applying the matching conditions from equation ( 3.35 ), the error dynamics can also be written as

$$\dot{e} = A_m e + L^{*-1}\left[-\tilde{K}x + \tilde{L}(A_m e + \dot{x}_d)\right] \qquad (3.38)$$

Suppose that $L^*$ is known to be either positive definite or negative definite. Let $\eta=1$ if $L^*$ is positive definite, and $\eta=-1$ if $L^*$ is negative definite. The matrix $\Gamma$ is then defined so as to always be a positive definite matrix.

$$\Gamma = inv(L^*)\eta \qquad (3.39)$$

The following positive definite Lyapunov candidate function is proposed

$$V = e^{\mathrm{T}}Pe + tr\left[\tilde{K}^T\Gamma\tilde{K} + \tilde{L}^T\Gamma\tilde{L}\right] \qquad (3.40)$$

where $P$ is a symmetric, positive definite matrix whose existence is guaranteed as a solution to

$$A_m^T P + PA_m = -Q \qquad (3.41)$$

where $Q$ is an arbitrary symmetric, positive definite matrix and $A_m$ is the previously selected Hurwitz matrix. By construction, the Lyapunov candidate is radially unbounded and decrescent. For a time invariant matrix $A_m$, the derivative of the Lyapunov candidate is

$$\dot{V} = \dot{e}^{\mathrm{T}}Pe + e^T P\dot{e} + \frac{d}{dt}tr\left[\tilde{K}^T\Gamma\tilde{K} + \tilde{L}^T\Gamma\tilde{L}\right] \qquad (3.42)$$

Substituting the error dynamics from equation ( 3.31 ) into ( 3.42 ) yields

$$\dot{V} = \left(A_m e + L^{*-1}\left[-\tilde{K}x + \tilde{L}(A_m e + \dot{x}_d)\right]\right)^T Pe$$
$$+ e^T P\left(A_m e + L^{*-1}\left[-\tilde{K}x + \tilde{L}(A_m e + \dot{x}_d)\right]\right) + \frac{d}{dt}tr\left[\tilde{K}^T\Gamma\tilde{K} + \tilde{L}^T\Gamma\tilde{L}\right] \qquad (3.43)$$

Using the properties of the trace outlined previously, equation ( 3.43 ) can be simplified as

$$\dot{V} = e^T(A_m^T P + PA_m)e + 2e^T PL^{*-1}\left[-\tilde{K}x + \tilde{L}(A_m e + \dot{x}_d)\right] + \frac{d}{dt}tr\left[\tilde{K}^T\Gamma\tilde{K} + \tilde{L}^T\Gamma\tilde{L}\right] \qquad (3.44)$$

$$\frac{d}{dt}tr\left[\tilde{K}^T\Gamma\tilde{K} + \tilde{L}^T\Gamma\tilde{L}\right] = 2tr\left[\tilde{K}^T\Gamma\dot{\hat{K}} + \tilde{L}^T\Gamma\dot{\hat{L}}\right] \qquad (3.45)$$

Equation ( 3.44 ) can be further simplified by substituting equation ( 3.41 ).

$$\dot{V} = -e^T Q e + 2e^T P L^{*-1}\left[-\tilde{K}x + \tilde{L}(A_m e + \dot{x}_d)\right] + 2tr\left[\tilde{K}^T \Gamma \dot{\hat{K}} + \tilde{L}^T \Gamma \dot{\hat{L}}\right] \qquad (3.46)$$

Two additional relationships can be derived using the properties of the trace function.

$$e^T P L^{*-1}\tilde{K}x = tr\left(\tilde{K}^T L^{*-1} P e x^T\right) \qquad (3.47)$$

$$e^T P L^{*-1}\tilde{L}(A_m e + \dot{x}_d) = tr\left(\tilde{L}^T L^{*-1} P e (A_m e + \dot{x}_d)^T\right) \qquad (3.48)$$

Substituting equations ( 3.47 )and ( 3.48 ) into equation ( 3.46 ) gives

$$\dot{V} = -e^T Q e + 2tr\left[\tilde{K}^T \Gamma \dot{\hat{K}} + \tilde{L}^T \Gamma \dot{\hat{L}} - \tilde{K}^T L^{*-1} P e x^T + \tilde{L} L^{*-1} P e (A_m e + \dot{x}_d)^T\right] \qquad (3.49)$$

The following adaptive update laws are chosen to make the Lyapunov candidate negative semi-definite

$$\dot{\hat{K}} = P e x^T sign(\eta) \qquad (3.50)$$

$$\dot{\hat{L}} = -P e (A_m e + \dot{x}_d)^T sign(\eta) \qquad (3.51)$$

$$\dot{V} = -e^T Q e \leq 0 \qquad (3.52)$$

### 3.2.3   Proof Of Stability

From $V \geq 0$ and $\dot{V} \leq 0$, V(t) is lower bounded and decreasing, which gives $V \in L_\infty$. Because $V \in L_\infty$, it is known that $e, \tilde{K}, \tilde{L}, \hat{K}, \hat{L} \in L_\infty$ because all signals comprising an $L_\infty$ signal must also be $L_\infty$. From $V \in L_\infty$ it is also true that $\lim_{t\to\infty} V(t) = V_\infty$ exists and is finite. The error signal e can be shown to be L₂ because $\lim_{t\to\infty} \int_0^t \dot{V}(\tau)d\tau = \lim_{t\to\infty} \int_0^t -e^T Q e \, d\tau = V(0) - V_\infty$. Since $e \in L_\infty, x \in L_\infty$ for the same reasons previously outlined. Since it has been shown that all elements of u are $L_\infty$, $u \in L_\infty$ as well. For the same reason, $\dot{e} \in L_\infty$. Since $e \in L_2 \cap L_\infty$ and $\dot{e} \in L_\infty$, by Barbalet's lemma $\lim_{t\to\infty} e(t) = 0$. The control input and adaptive update laws guarantee

that all signals and states remain bounded and that the tracking error asymptotically approaches 0.

### 3.2.4 Definiteness of Matrix L

It still remains to be shown that the matrix $L$ is guaranteed to be either positive or negative definite. In the case of combined FWS and DYC control, the input matrix $B$ is given by

$$B = \begin{bmatrix} \dfrac{2C_f}{mV} & 0 \\ \dfrac{2C_f L_f}{I_z} & \dfrac{1}{I_z} \end{bmatrix}$$

(3.53)

Since $B$ is square, $L$ is found simply by inverting $B$.

$$L = \begin{bmatrix} \dfrac{mV}{2C_f} & 0 \\ -L_f mV & I_z \end{bmatrix}$$

(3.54)

Since the vehicle inertia, mass, and tire cornering stiffness are always positive, the matrix $L$ will be positive definite for all positive velocities, and negative definite for all negative velocities. Since the controller is only expected to be operating in positive velocities, $L$ will be taken as positive definite for the remainder of the paper.

In the case of four wheel steering control,

$$B = \begin{bmatrix} \dfrac{2C_f}{mV} & \dfrac{2C_r}{mV} \\ \dfrac{2C_f L_f}{I_z} & -\dfrac{2L_r C_r}{I_z} \end{bmatrix}$$

(3.55)

Inverting this to find $L$ yields

$$L = \begin{bmatrix} \dfrac{L_r mV}{2(C_f L_f + C_f L_r)} & \dfrac{I_z}{2(C_f L_f + C_r L_r)} \\ \dfrac{L_f mV}{2(C_r L_f + C_r L_r)} & -\dfrac{I_z}{2(C_f L_f + C_r L_r)} \end{bmatrix}$$

(3.56)

Definiteness of L is determined by checking the signs of the leading principal minors. That is to say, the upper left element and the determinant of L must share the same sign.

$$\det(L) = -\frac{I_z mV}{4C_f\left(C_r L_f + C_r L_r\right)}$$
( 3.57 )

The sign of $L_{1,1}$ and det(L) are seen to be sgn(V) and −sgn(V), respectively. Since the leading principal minors are neither both positive, nor both negative, L is neither positive nor negative definite. The implication of this is that adaptive control by this approach is not possible for a 4WS system. It may be possible to implement another form of adaptive control, such as adaptive pole placement or an ANFIS system, but such research is left for future work.

### 3.3 TIRE SLIP CONTROLLER

In order to implement direct yaw control, the longitudinal forces on the driving tires must be specified. The tire rotational dynamics are given by

$$I_w \dot{\omega}_{ij} = -R_w F_{xij} + T$$
( 3.58 )

where $T$ is the torque exerted by the tire slip controller, $F_{xij}$ refers to the longitudinal force generated by tire slip, and $R_w$ is the wheel radius. Rolling resistance has been neglected due to its small effect in the overall dynamics. The dynamic tire model is shown below in Figure 3.16.
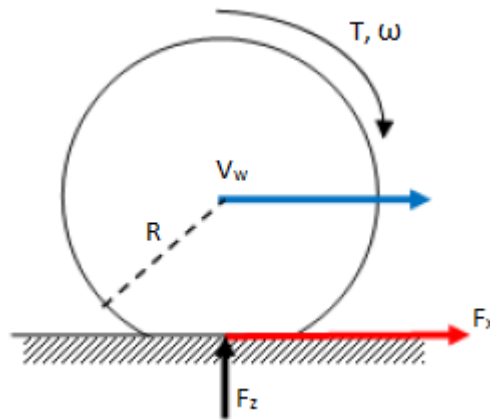


Figure 3.16 Simplified tire dynamic model

To specify the longitudinal force, the tire slip must be controlled. A low level controller is developed to achieve the longitudinal slip required to generate the requested force. The Pacejka magic formula is again used as the tire model. First, a lookup table is generated based on the normal force present on the tire and current system state. Given the requested force, a required longitudinal slip is returned and the necessary rotational velocity of the wheel is calculated. This rotational velocity is then used as the reference velocity for the tire controller. A simple PI controller is used to drive the wheel to a desired slip state by controlling the motor torque. In the first round of modeling it is assumed that the engine is capable of providing the required torque without limitations. Later iterations of the model include transient response and saturation of the engine torque to values seen in a high performance vehicle. The effects of changing the motor model can be seen in section 4.3.2 in the following chapter.

The technique used in this thesis is purely a proof of concept method, as it assumes knowledge of parameters that cannot easily be measured, such as road surface conditions. More robust tire slip controllers have been developed for similar purposes. [Wang & Longoria, 2006] develops a combined longitudinal and lateral slip controller to optimally distribute tire loads for vehicle stability. Their work uses the Pacejka magic formula as the tire model and a nonlinear sliding mode controller. It has been shown to be more effective than traditional DYC techniques in a split-mu braking condition. [Liang, et al., 2009] develops an adaptive tire slip controller for yaw moment generation. Their research uses the LuGre tire model and assumes that the road friction coefficient is an unknown parameter. The controller seeks to drive the wheels to the optimal combined longitudinal and lateral slip condition. [Canudas & Tisotras, 1999] also use the LuGre model in combination with a sliding mode controller to achieve the desired longitudinal tire forces. [Hsiao, 2013] develops a tire force controller through the use of an observer that is robust to parameter uncertainties and combined tire slip conditions. Hsiao uses the Dugoff tire model for controller design and the Pacejka model for controller validation. Production vehicles that implement DYC through ABS or other forms of TCS simply seek to maximize the tire longitudinal force by aiming for the slip value with peak force [Liang, et al.,

2009]. Liang notes that this model does not necessarily generate the maximum yaw moment, as it doesn't account for the combined slip condition.

# Chapter 4: Controller Validation

In this chapter, the controller is validated on several models of increasing complexity. The results are first shown for the application of the controller to the linear model for which it was designed. This acts as a proof of concept for the controller's ability to stabilize a previously unstable system. The controller is then applied to the nonlinear handling model developed in section 2.1. The addition of the nonlinear tire effects allows us to see the limitations of an uncontrolled vehicle on slick surfaces. The results of the nonlinear handling validation showed that there may be further implementation issues associated with the saturation and lag present in an actual electric motor. This prompted the addition of a simple motor model and the use of a filtered output on the controller yaw moment in an attempt to reduce the required motor torque. Unless otherwise specified, all tests were performed at 22.35 m/s (50 mph) with no external disturbances. The vehicle was commanded to make a double lane change with a steering angle of 3 degrees.

## 4.1 VALIDATION USING LINEAR HANDLING MODEL

As a proof of concept, the controller is applied to the linear system model for which it was developed. No tire saturation limits were imposed, and constant forward velocity was assumed. The 4WS and FWS+DYC controllers were given the correct parameter values, and the adaptive controller was given initial errors of -20% for the values of K and L. The controller was tested on both a directionally stable and directionally unstable vehicle as predicted by the Rocard stability analysis.

### 4.1.1 Directionally Unstable System

First, the controller was tested on a directionally unstable system. The system was controlled using the combined FWS and DYC approach, the adaptive FWS and DYC controller, and a 4WS controller for comparison. As seen in Figure 4.17, the uncontrolled system is unable to perform the requested maneuver and increasingly deviates from the desired path. All three

controllers are able to drive the tracking error to zero and keep the side slip angle within an acceptable range.
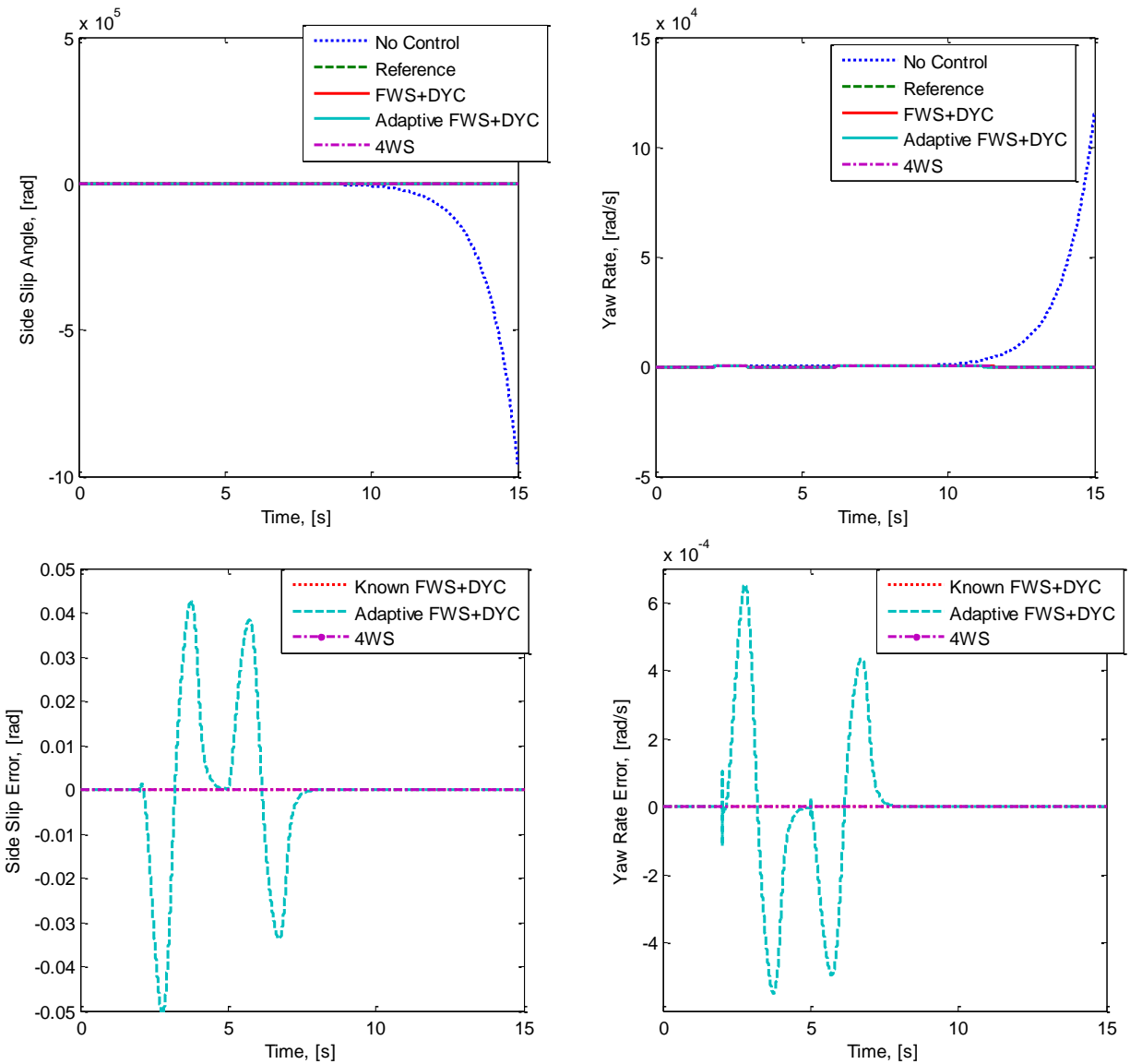


Figure 4.17 System states and tracking error for an unstable linear system

The controller inputs are shown in Figure 4.18. The requested yaw moment is slightly larger than is physically realizable, but this can be remedied by varying the controller tuning to place a larger load on the front wheels. The high frequency nature of the requested front wheel steering angle in the adaptive case may also prove difficult to implement in a physical system.
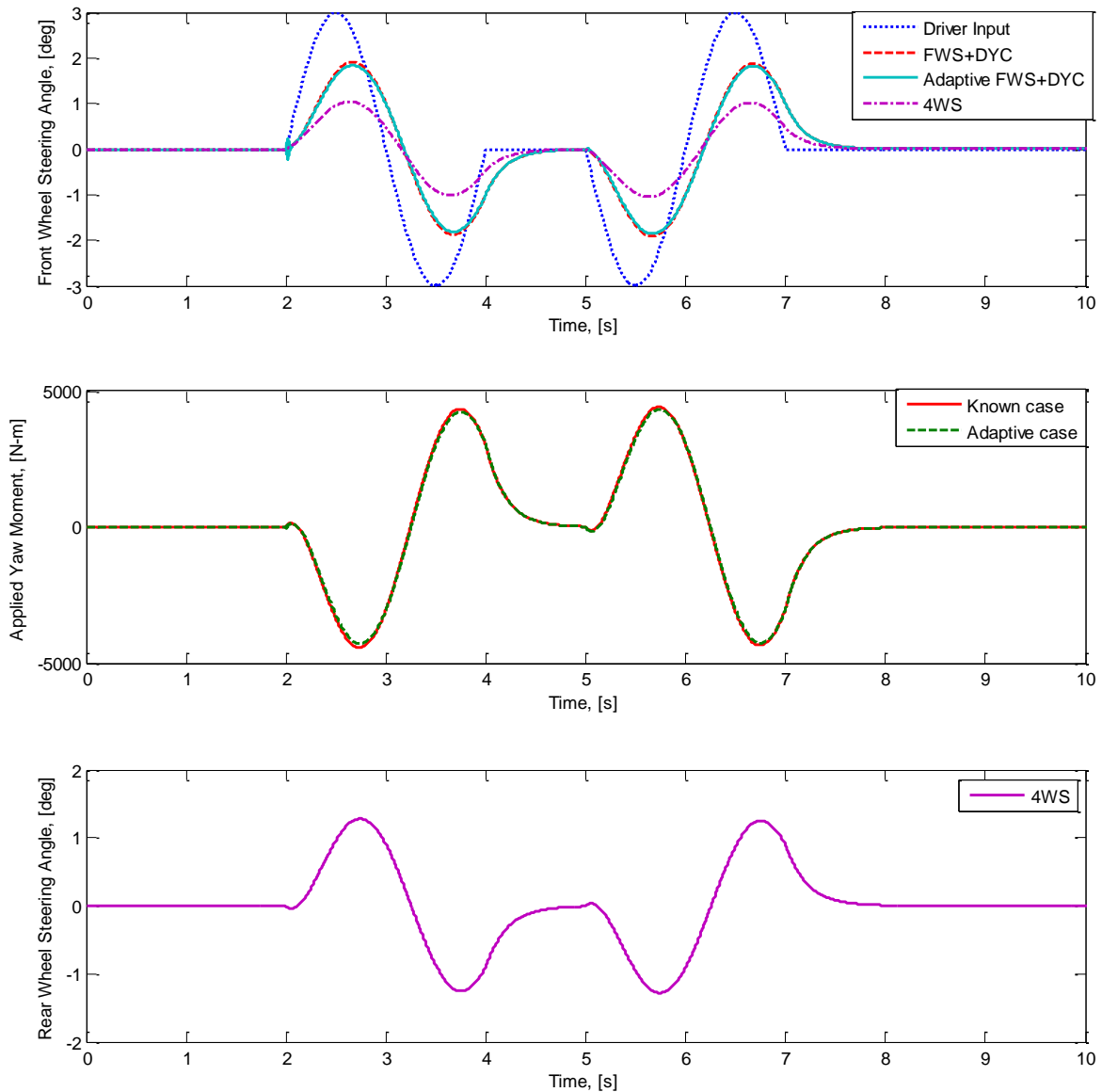
Figure 4.18 Controller inputs for an unstable linear system

The parameter estimates in the adaptive case are shown in Figure 4.19. Though the estimates do not converge to the actual parameter values, they do reach finite steady state values. During testing, issues arose in finding appropriate parameter update gains. If the values of K and L are computed from the known values, it can be seen that the different elements vary by several orders of magnitude. This makes it difficult to select a set of matrices $A_m$ and $Q$ that

allow the largest elements to substantially change without driving the smallest elements to instability.
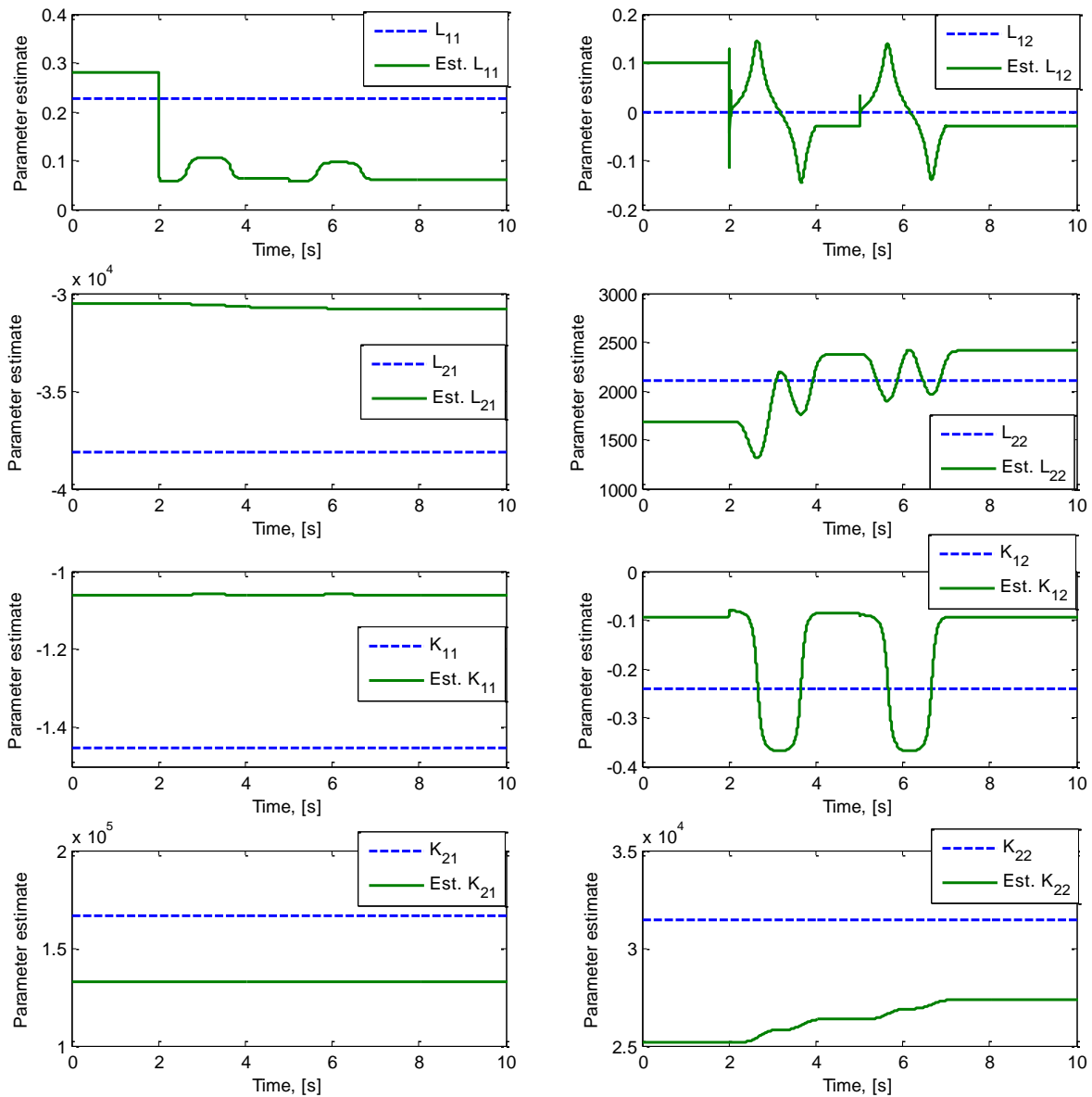


Figure 4.19 Adaptive parameter estimates for an unstable linear system

### 4.1.2    Directionally Stable System

The controllers are also tested on a directionally stable system to investigate their effect on a typical driving experience. The purpose of this is to make sure that the controllers do not give the driver the impression that the vehicle is less responsive with the controllers than

without. The controllers used in this test are given the same tuning as those in the previous section.

The results in the following figures show that all three controllers closely track the desired yaw rate and side slip angle. The reference model does give a lower yaw rate than the uncontrolled system, but with a decreased side slip angle.
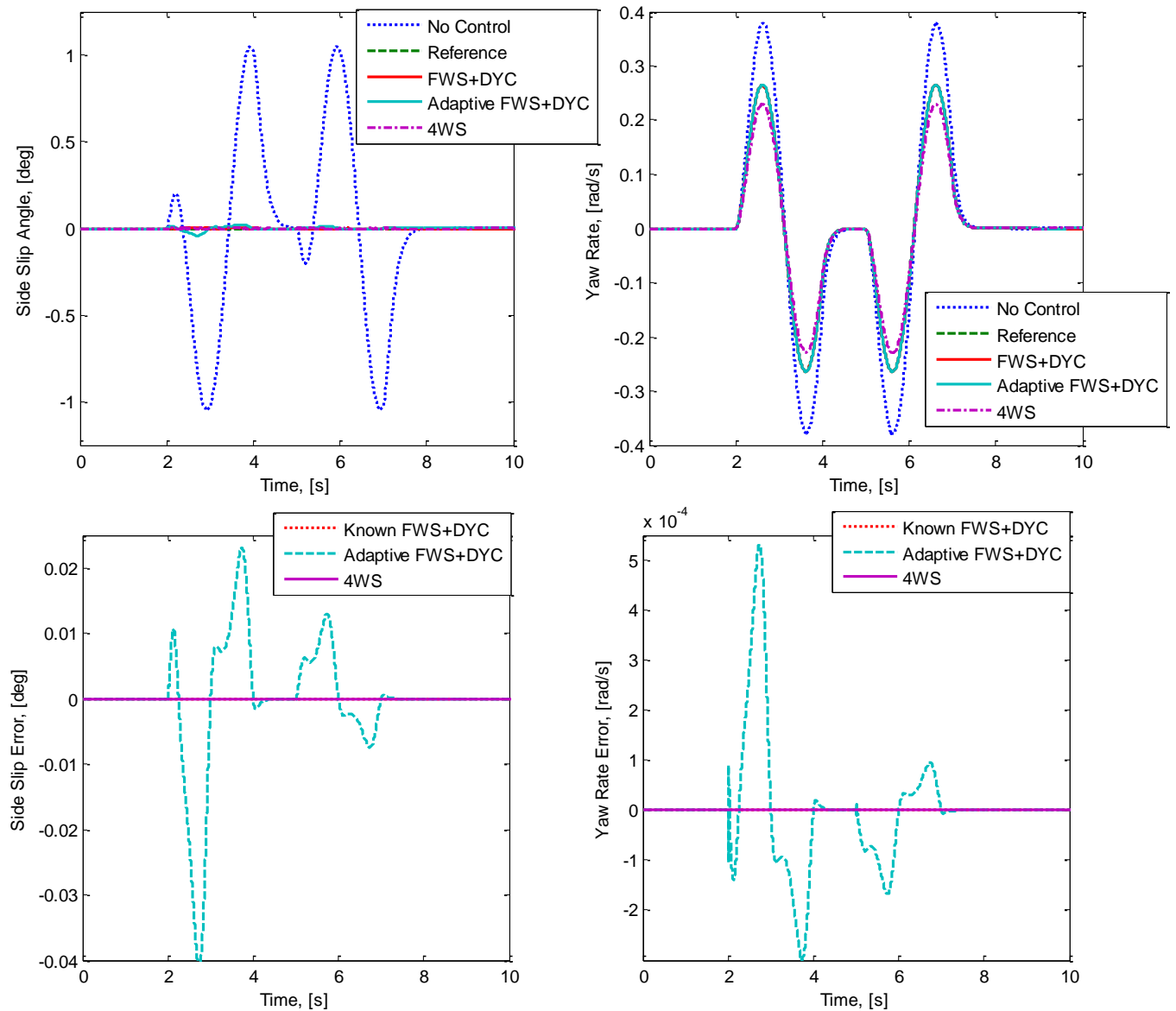


Figure 4.20 System states and tracking error for a stable linear system

As in the directionally unstable case, the adaptive controller gives a high frequency control input on the front wheel steering angle that is unlikely to be realizable in a physical system. The adaptive parameter estimates show behavior similar to what was seen previously in Figure 4.19.
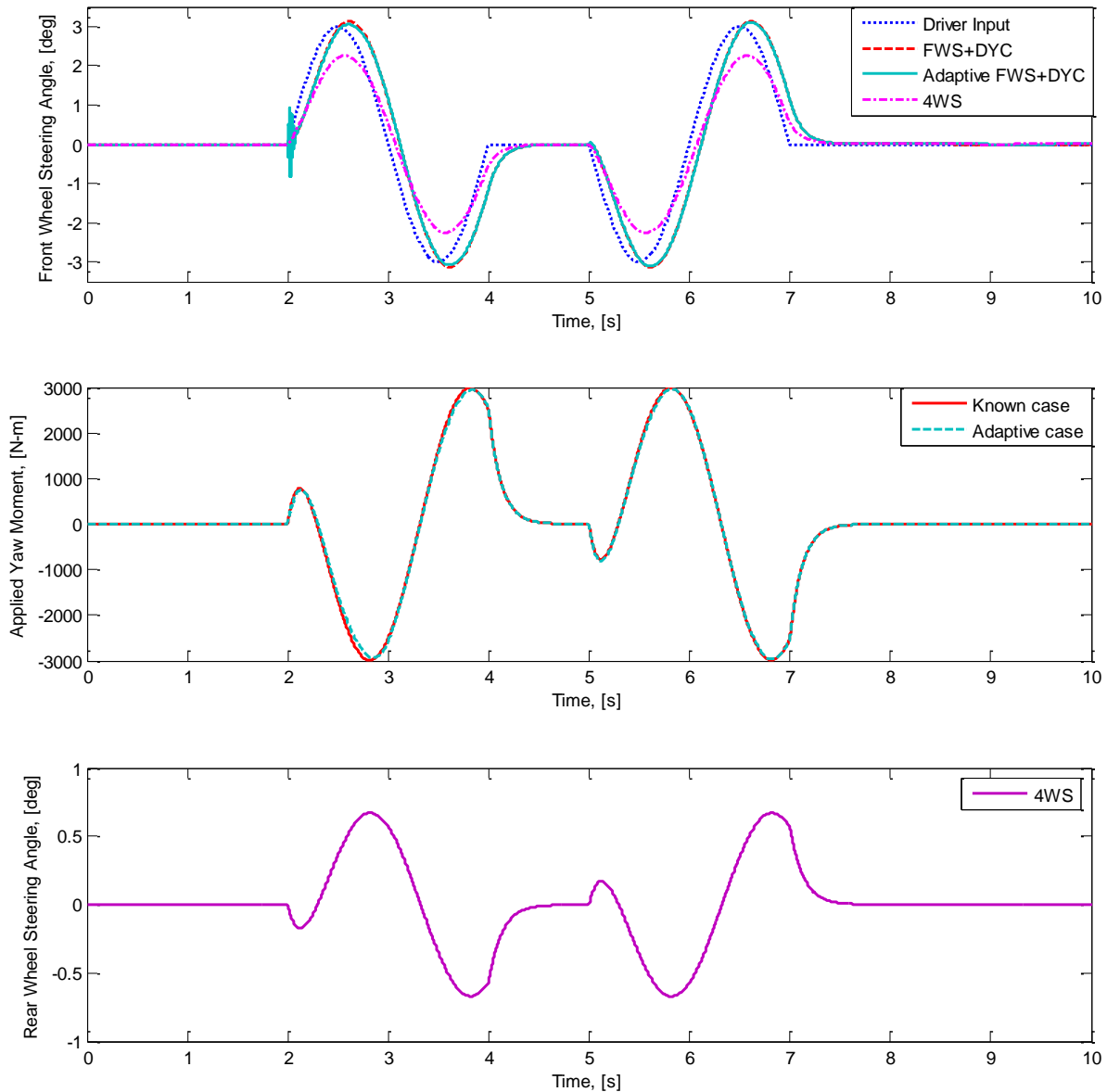


Figure 4.21 Controller inputs for a stable linear system

## 4.2 VALIDATION USING 2D NONLINEAR MODEL

In the second round of testing, the controller was applied to the nonlinear handling model developed in section 2.1. The yaw moments commanded by the controller were

49

converted to longitudinal forces of equal magnitude on the rear left and rear right tires. The tire and motor dynamics were neglected, and the system was simulated as though the tire achieved the required slip angle instantaneously. The effect of the combined slip condition on the rear tires was accounted for when calculating the available longitudinal and lateral forces.

### 4.2.1 Low friction Double Lane Change with Parameter Error

In this simulation, the mass and inertia of the vehicle were both increased by 30%. This caused changes in the tire stiffness as predicted by the tire lateral force equations developed in section 2.2.1. The controller parameters and reference model were calculated using the pre-loading values for mass, inertia, and tire stiffness. The double lane change maneuver is performed on a slick road with a coefficient of friction $\mu = 0.4$. Though the uncontrolled system states shown in Figure 4.22 do not immediately indicate instability, the global coordinates plotted in Figure 4.23 show that the uncontrolled system is unable to perform the requested maneuver. All three controllers are able to prevent the system from excessive sliding, though with offsets in the global Y direction. These offsets could potentially be accommodated by slight driver interventions. The adaptive control law does not appear to improve the behavior of the vehicle over the non-adaptive case.
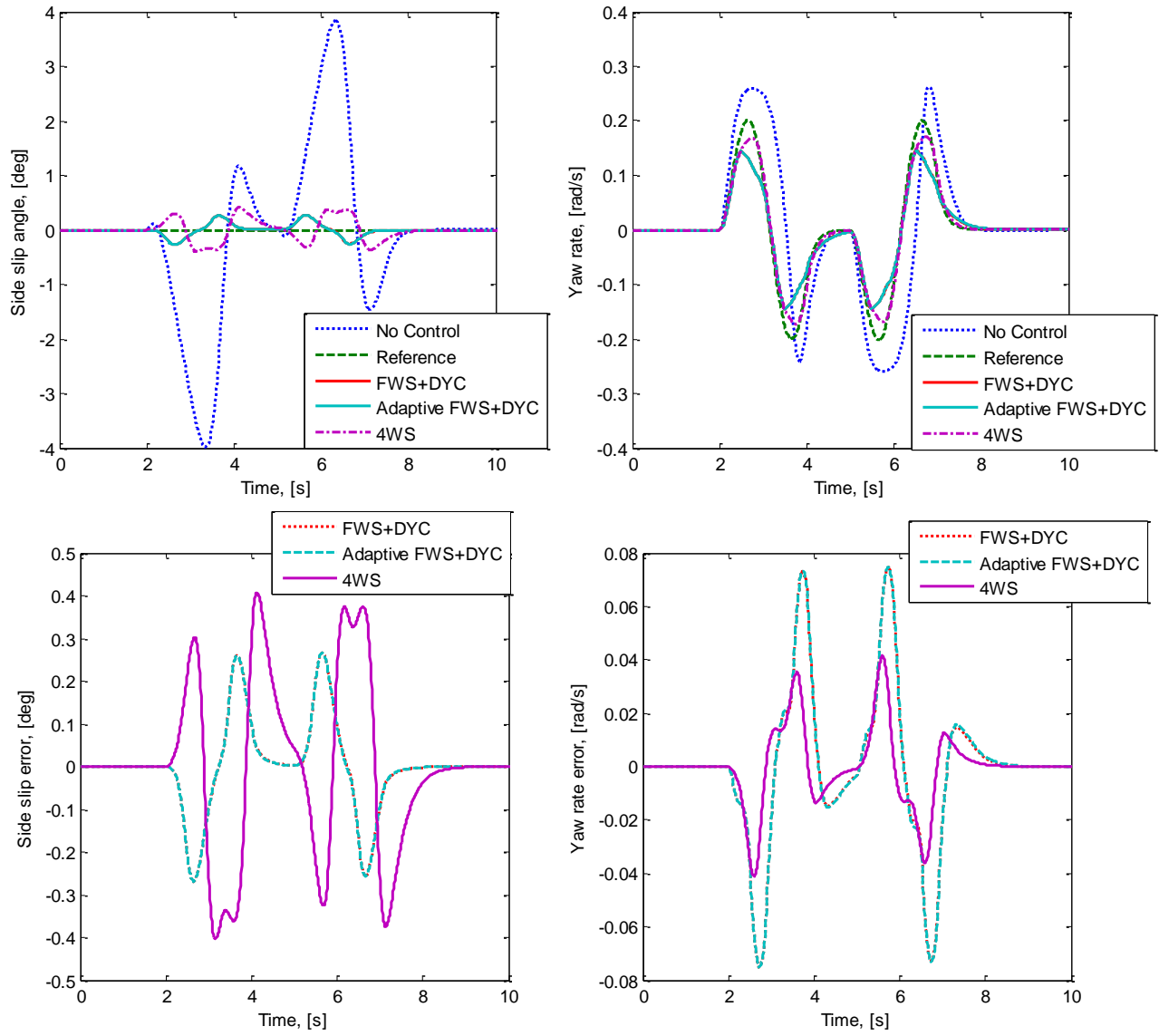
Figure 4.22 System states and tracking errors for a low friction nonlinear system
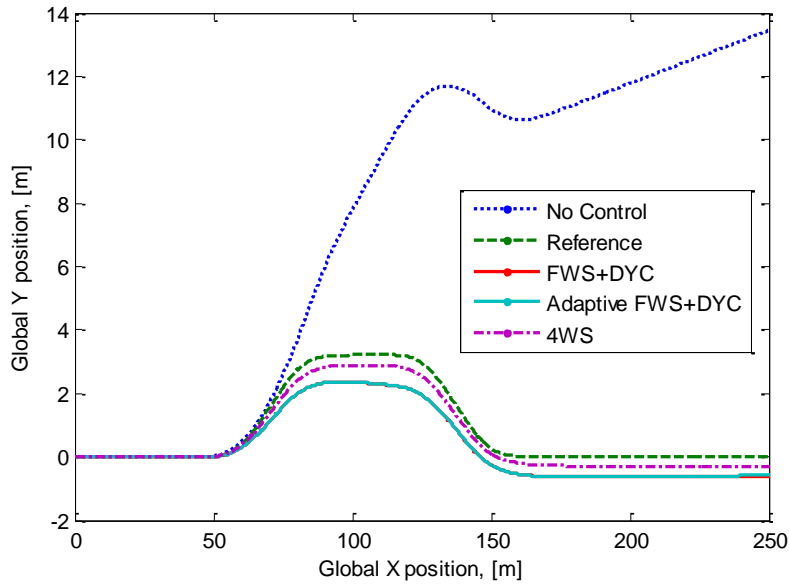
Figure 4.23 Vehicle global position for a low friction nonlinear system

The controller inputs of the adaptive case do not demonstrate the same high frequency effects seen in the linear model simulation. Additionally, the yaw moment interventions are made smaller by tuning the controller to exert more of the required force using the front wheel steering angle. The yaw moments shown are those commanded by the high level controller. When the commanded yaw moment exceeds the tractive limits of the tires, the low level controller saturates the output to the maximum realizable value and commands the tires to the corresponding longitudinal slip. The desired yaw moments seen in the second row of Figure 4.24 give rise to concerns about the implementation of this control scheme. At several points during the maneuver, the commanded yaw moment changes sharply, which could require a very large torque input to achieve. Such sharp changes will also be inhibited by the inertia of the tire as it is driven to the appropriate rotational velocity.
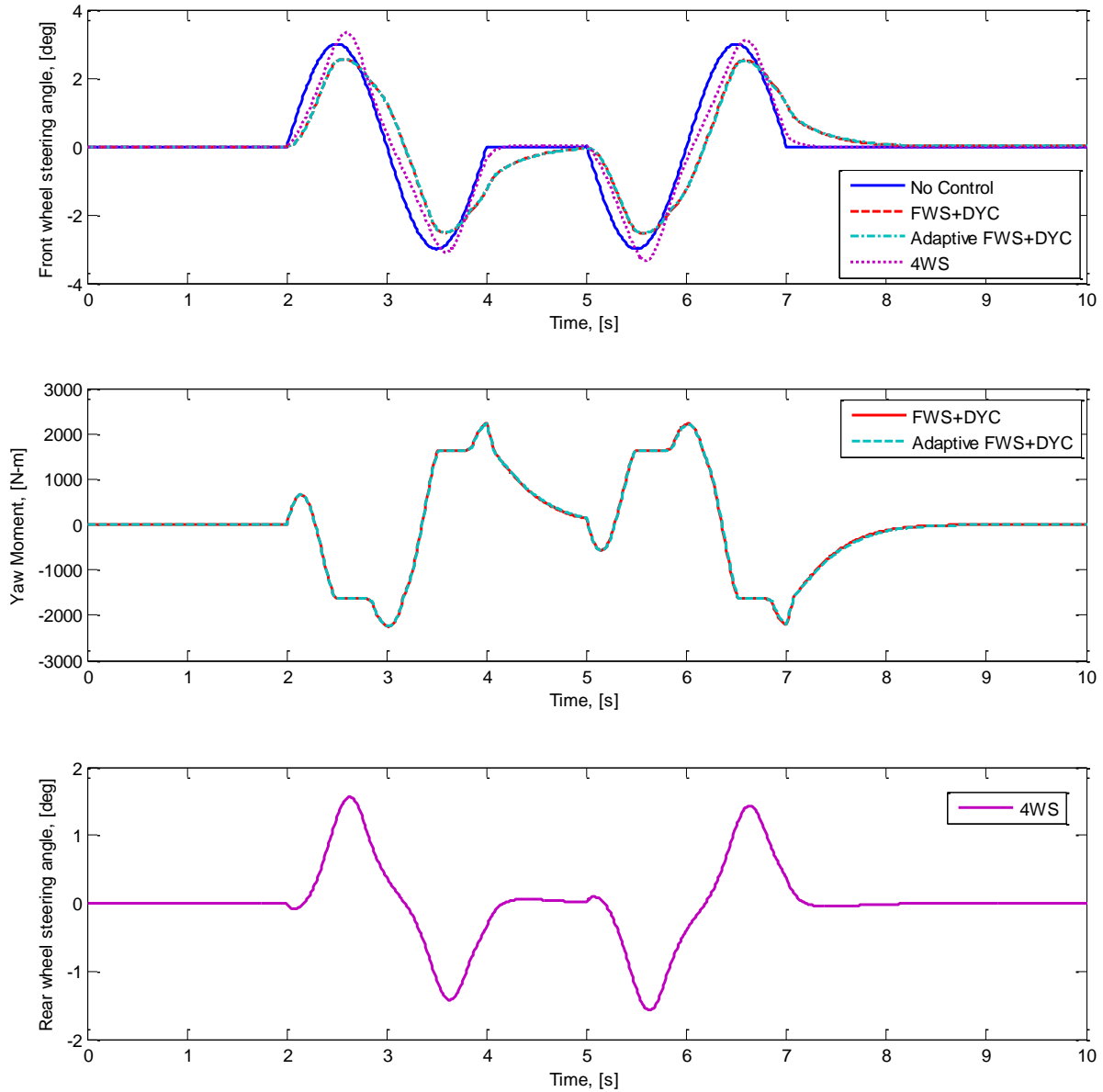
Figure 4.24 Controller inputs for a low friction nonlinear system

Though the yaw rate is decreased in the controlled vehicle, the driver is able to maintain a higher forward velocity while remaining on a stable trajectory. The system longitudinal and lateral velocities are shown below in Figure 4.25. Both the combined FWS+DYC and 4WS controllers show improvements over the uncontrolled case.
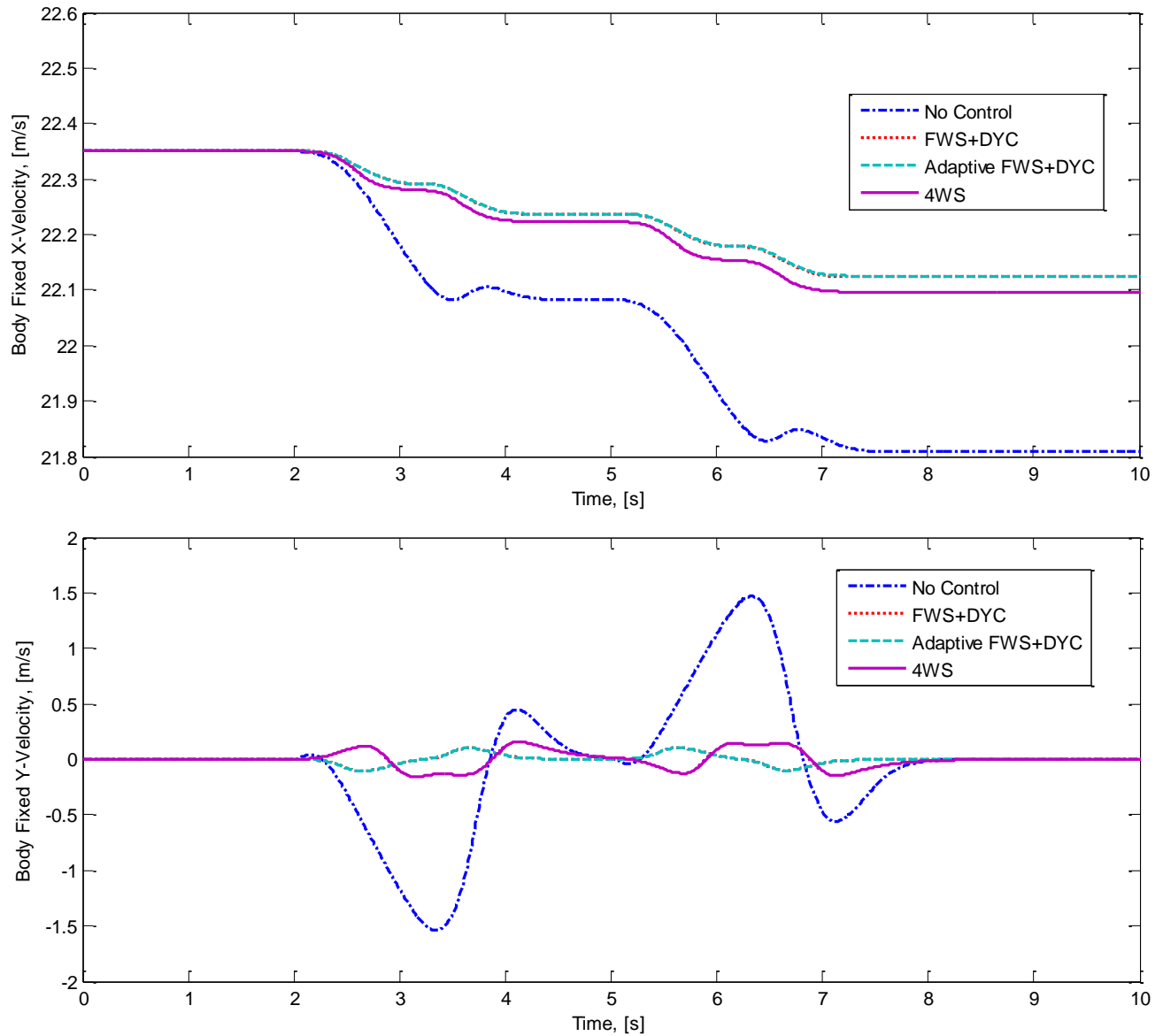
Figure 4.25 Longitudinal and lateral velocities for a low friction nonlinear system

As in the linear case, the adaptive parameter estimates do not reach the actual parameter values, but do eventually settle to constant, finite values. When the nonlinear elements of the model were included, it was found that significantly smaller adaptive update terms were required to maintain boundedness of the estimates. Because of this, only the smallest elements of the unknown terms were affected by the adaptive update laws.
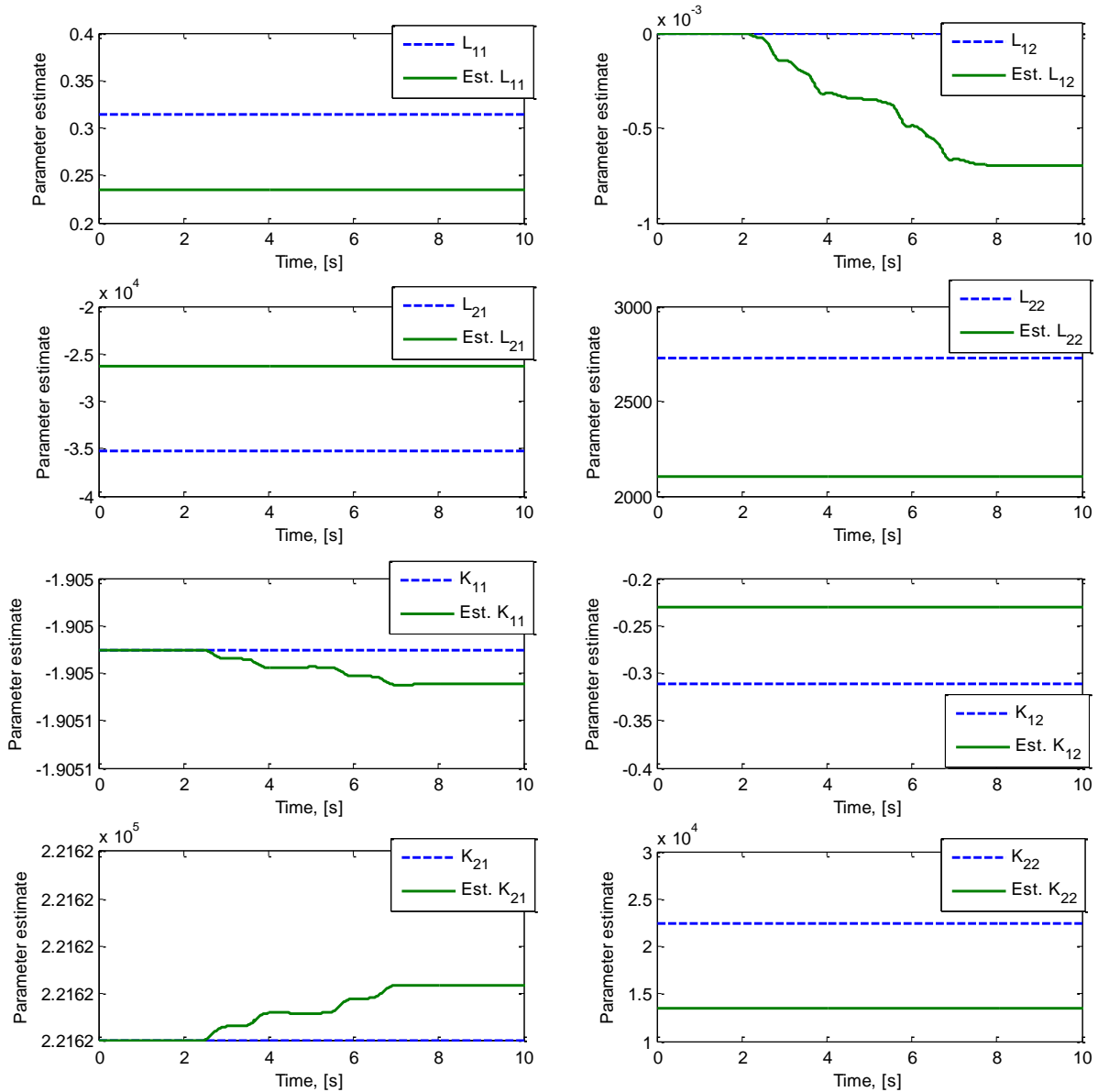
Figure 4.26 Adaptive parameter estimates for a low friction nonlinear system

## 4.2.2 Low Friction Double Lane Change without Parameter Error

In order to demonstrate the best possible performance of each controller, the results are also presented for the controllers without any parameter estimation error. The controllers all show improved response and achieve increased yaw rates with decreased side slip angles. This translated to a decrease in the global Y position offset during the maneuver.

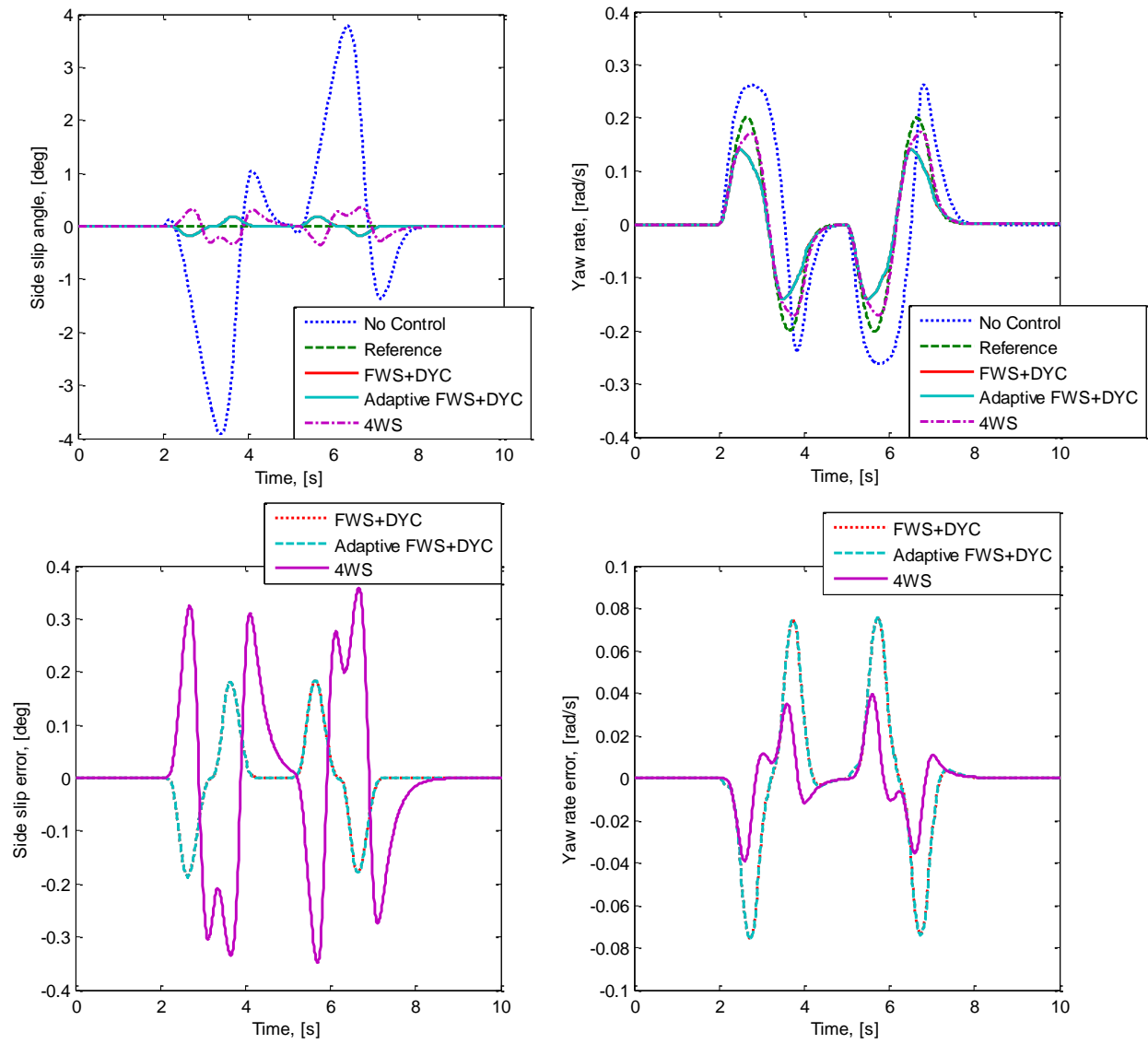Figure 4.27 System states and tracking errors for control without parameter estimation error
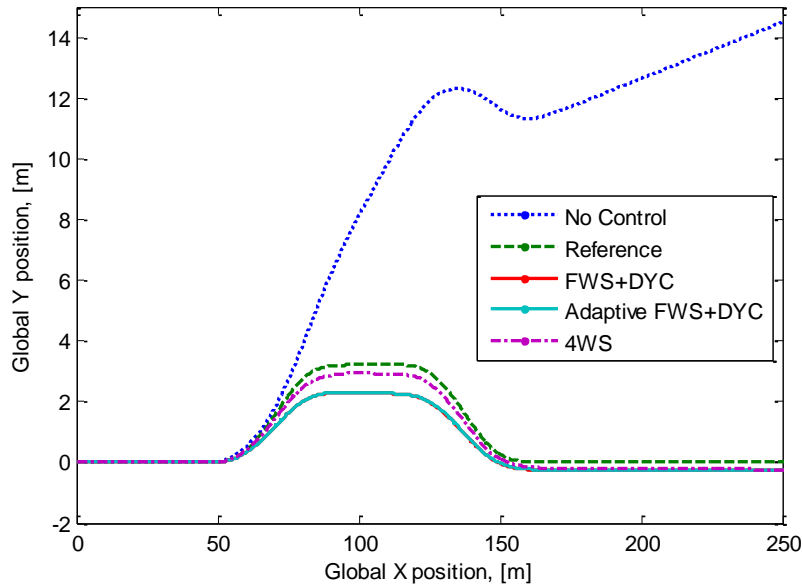
Figure 4.28 Vehicle global position for control without parameter estimation error

The remaining graphs are omitted, as the results are virtually identical to the previous case with parameter error.

**4.3 VALIDATION USING 2D NONLINEAR MODEL AND TIRE SLIP CONTROL**

In this section, the complexity of the actuator model is again increased. Rather than specifying tire longitudinal forces directly, the longitudinal slip required to generate the desired forces is calculated and used as an input to the simple tire slip controller developed in section 3.3. First, the torque required to achieve the yaw moments generated in section 4.2.2 is shown. Then, the system response is presented for the case when motor torque is limited to a peak torque of 1000 Nm and a continuous torque of 500 Nm, as is available in the high performance Protean in-wheel motors [Protean, 2014]. The results presented are for the tests with parameter estimation errors.

It was found that the simplest method to provide the necessary torque to the driven tires would be to use an electric vehicle where the tires are individually driven. This conclusion is supported by the work of [Liang, et al., 2009], which suggests that in-wheel electric motors could improve the tire actuation rate and aid in the problem of unequal actuator rates caused

57

by faster responses in braking than driving. The in-wheel electric motor also gives the advantage of removing the inertia of the drive train, which reduces the torque required.

It was hypothesized that controller performance could be improved by low-pass filtering the yaw moment output of the high level controller. This could smooth out the rapid changes in yaw moment and further reduce the required motor torques. This approach was implemented in section 4.3.3.

### 4.3.1 Unregulated Motor Torque

Figure 4.29 shows the longitudinal slip and motor torque associated with the controller inputs presented in the low friction double lane change with parameter errors. Only one torque/slip profile is shown for each of the adaptive and non adaptive cases. The profile for the remaining tire is omitted, as the requested torque is equal in magnitude and only differs in direction. In both the adaptive and non-adaptive controller, the requested torque is significantly higher than what could be delivered by a vehicle motor. The high rate of change of the torque may also present implementation issues.

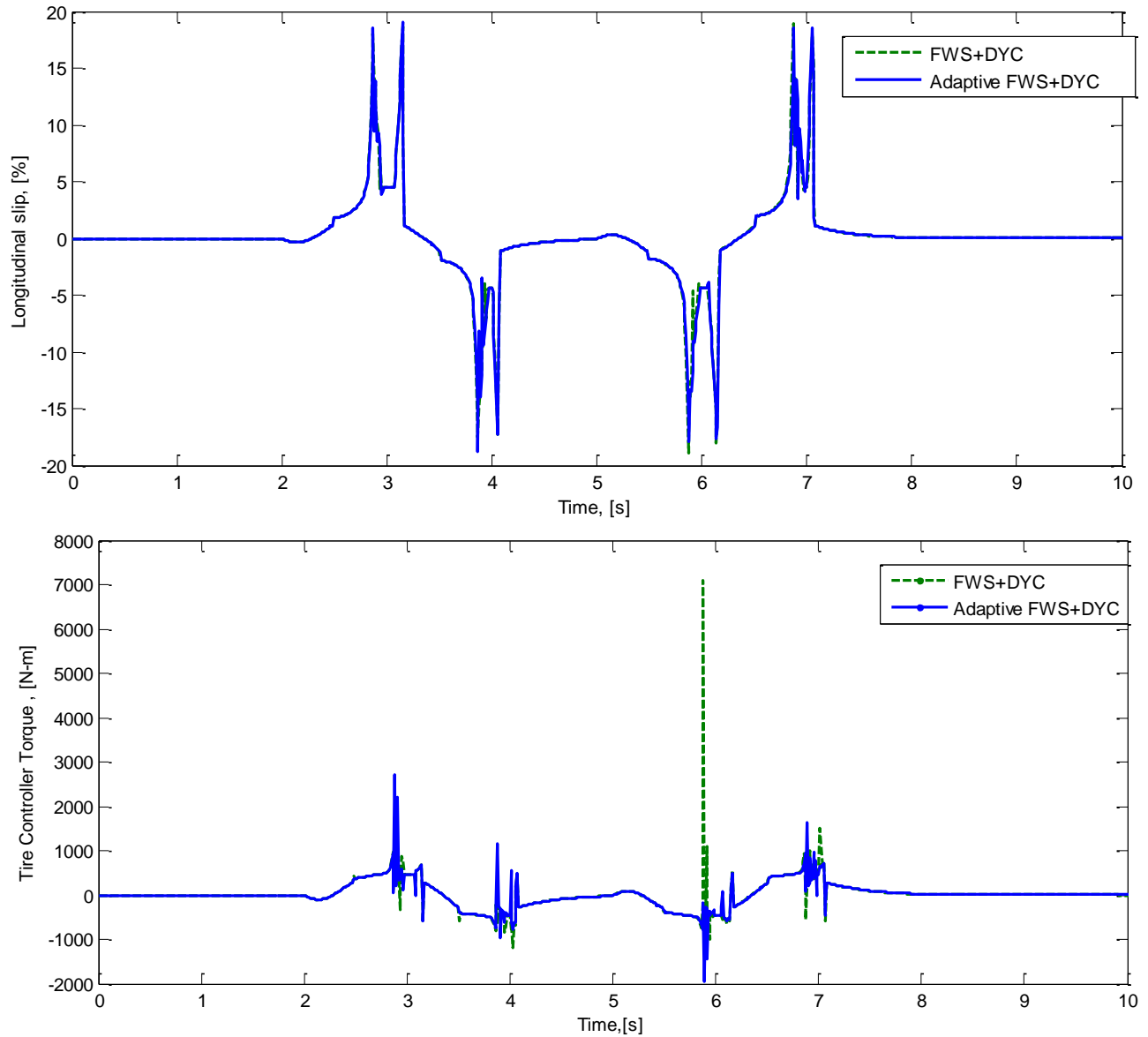Figure 4.29 Motor torque and tire slip angle for unregulated actuator

## 4.3.2 Limited Torque

The system is again simulated, this time with a saturated torque output and a dynamic motor model. Using the motor model presented in [Shino & Nagai, 2001] that neglects the dynamic effect of inductance, the motor torque output takes the form of a first order lag.

$$\dot{T} = \frac{R_m}{L_m}(T_{ref} - T) \tag{4.1}$$

Where $R_m$ and $L_m$ are the motor torque and inductance, $T_{ref}$ is the commanded torque from the tire slip controller, and T is the motor output torque. This model neglects the power-limiting effects of back EMF.

As seen in Figure 4.30 and Figure 4.31, the controller is able to stabilize the vehicle, though the Y-coordinate offsets from the previous trials still remain. As before, these could potentially be removed by driver intervention. The adaptive control law does not appear to provide any significant improvement over the non-adaptive case.
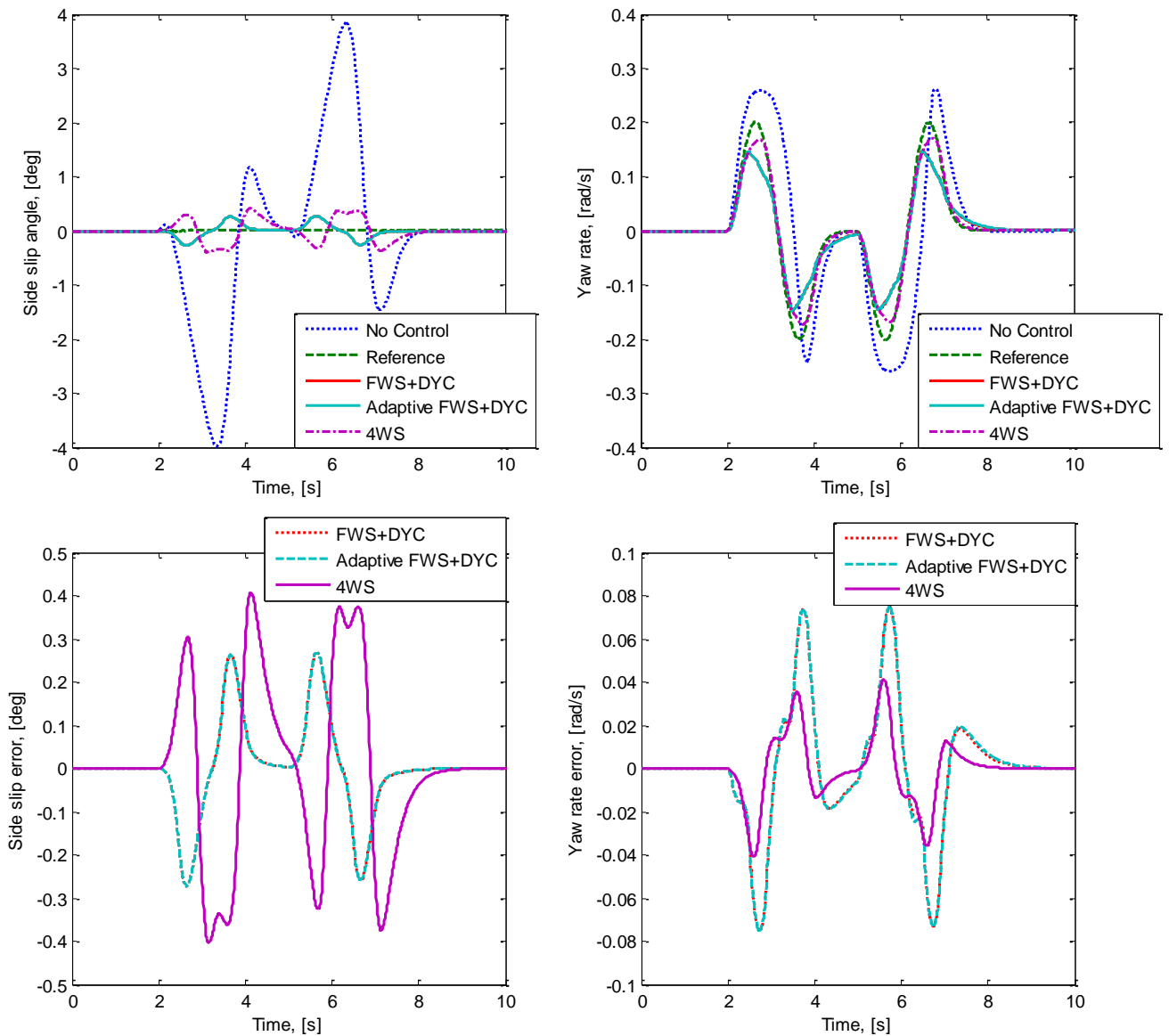


Figure 4.30 System states and errors for a nonlinear system with torque limited actuators
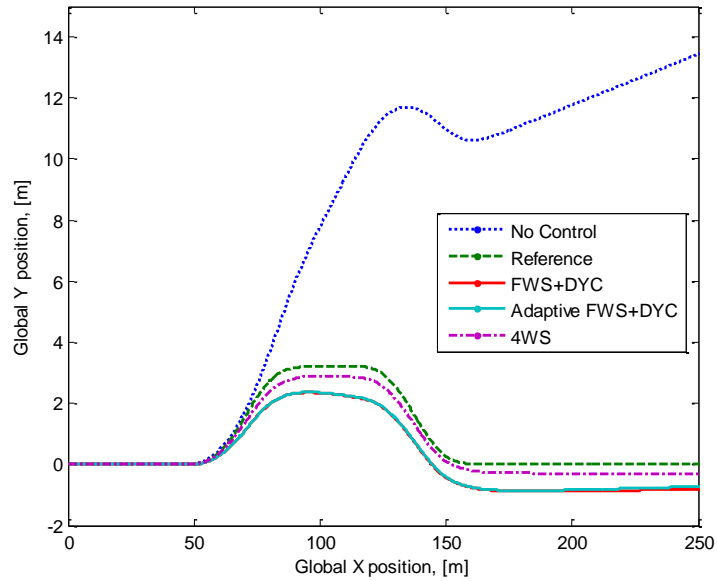
Figure 4.31 Vehicle global position for a low friction nonlinear system with torque limited actuators

The controller outputs and velocity profiles are largely unchanged from the previous trials, so their plots are omitted. An area of concern is now the rapid rate of change of the required motor torque and tire longitudinal slip, seen below in Figure 4.32. Though the vehicle is able to remain stable with these rapid changes, they may have unintended consequences on motor and tire life. The motor torque remains below the specified peak value, and is typically centered around the continuous torque listed in the motor specifications [Protean, 2014].

Figure 4.32 Motor torque and tire slip angle for torque limited actuators

### 4.3.3 Limited Torque and Filtered Yaw Moment

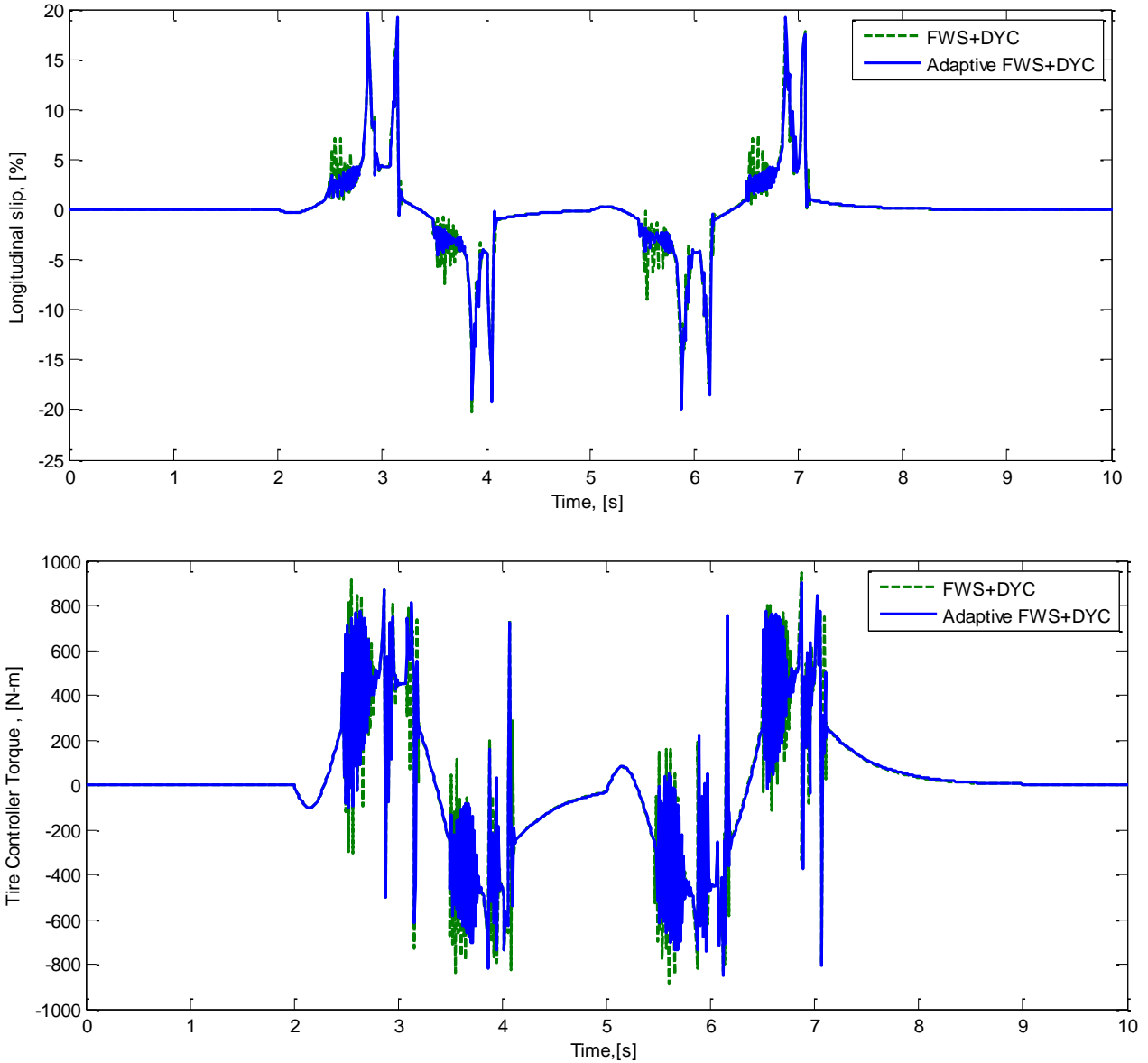In an attempt to alleviate the problem of the large, rapidly changing required torques, a simple first order low pass filter is applied to the controller yaw moment. The filter takes the form

$$\tau \dot{M}_f + M_f = M_{ref} \qquad (4.2)$$

Where $M_f$ is the filtered yaw moment, $M_{ref}$ is the output from the tire slip controller, and $\tau$ is the filter constant. By trial and error, it was found that a filter constant of $\tau = 10$ was the best tuning. It was also found that smaller filter constants, in the range of $\tau = 1$, can drive the vehicle to instability. A low pass filter applied to the tire slip controller torque was also considered, but was found to be ineffective when implemented alone or in conjunction with the yaw moment filter.

Figure 4.33 and Figure 4.34 show that the filtered yaw moment helps to reduce the tracking error of the DYC controller. As in the other trials, the adaptive parameter estimates do little to improve the performance of the vehicle.
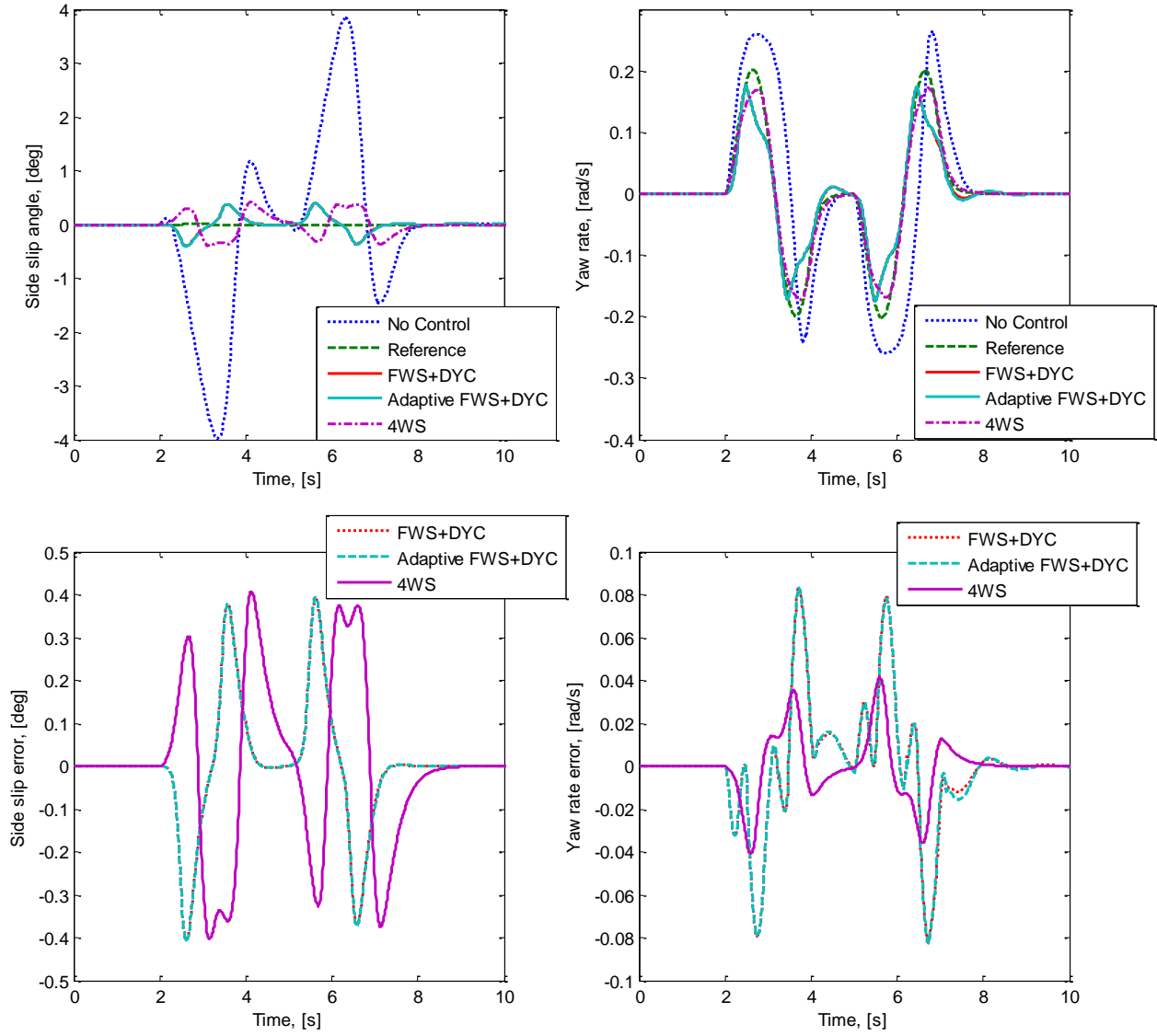
Figure 4.33 System states and errors for a nonlinear system with filtered control output
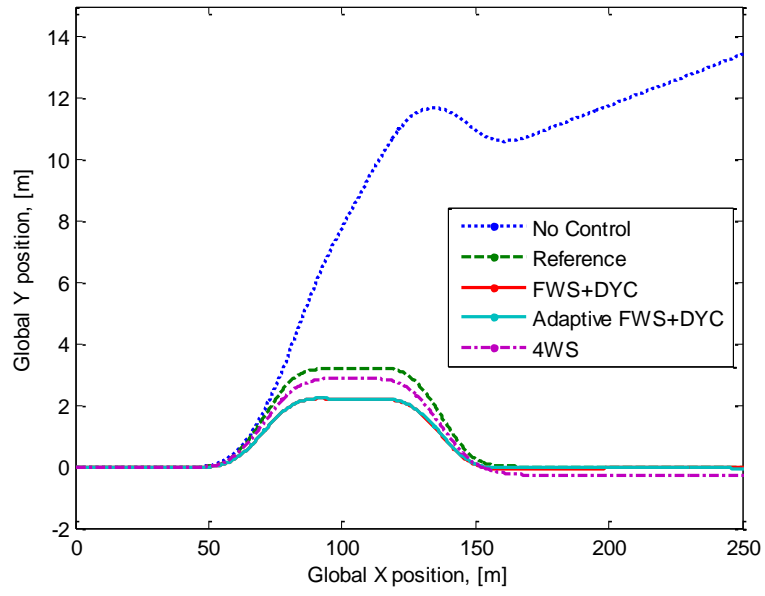
Figure 4.34 Vehicle global position for a low friction nonlinear system with filtered control output

The yaw moment filter successfully removes the sharp changes in the requested yaw moment, but the commanded yaw moment intervention is slightly larger than in the unfiltered case.
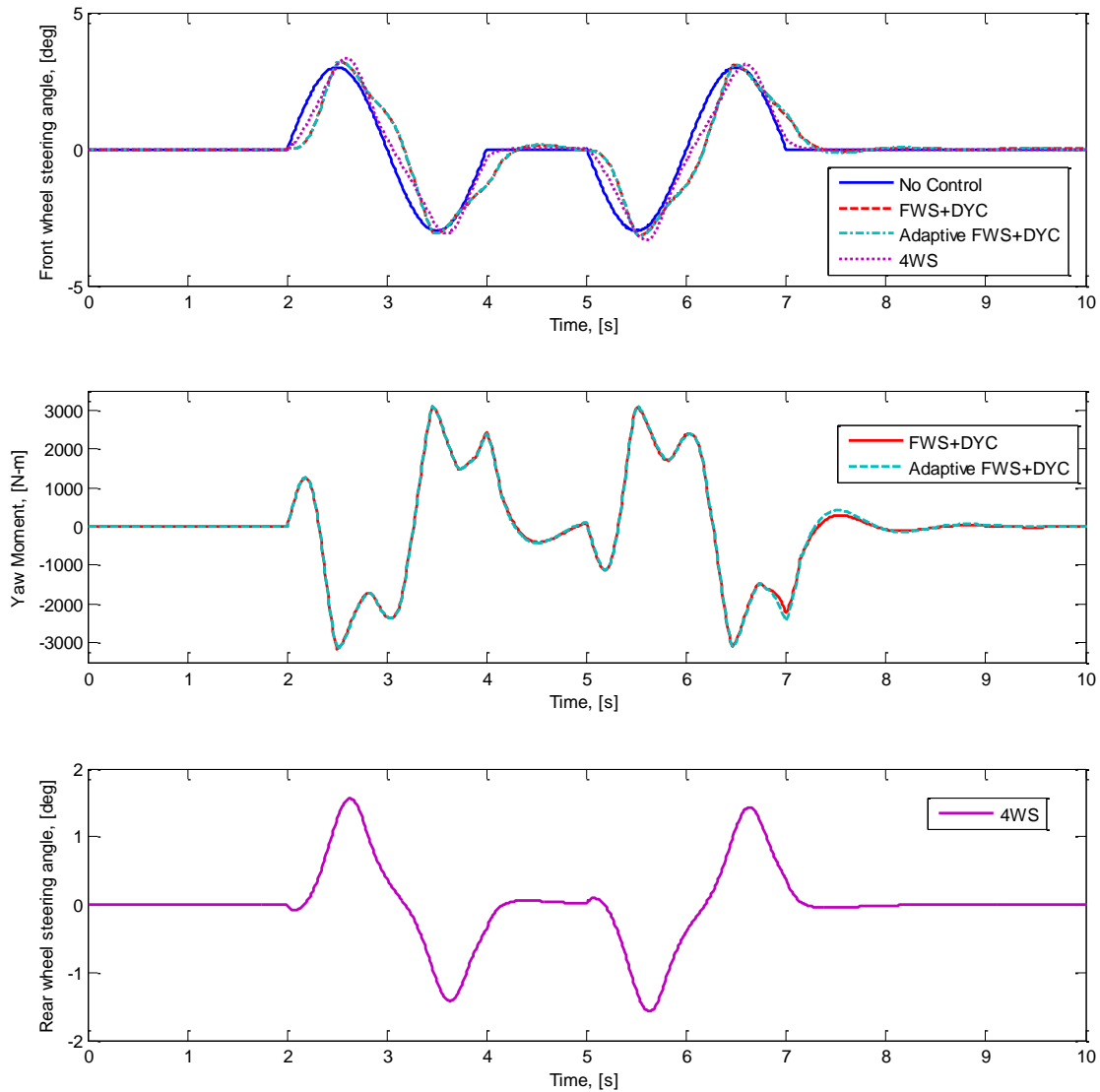


Figure 4.35 Controller inputs for a low friction nonlinear system with filtered control outputs

The motor torque again remaind beounded by the maximum allowable value and is centered about the available continuous torque. The high frequency content of the motor torque signal is reduced, but not entirely removed by the yaw moment filter.

Figure 4.36 Motor torque and tire slip angle for filtered controller outputs

# Chapter 5: Conclusions and Future Work

In this research, a model reference adaptive controller was developed for combined front wheel steering and direct yaw control. A Lyapunov approach was used for controller development and proof of stability. A simplified, bicycle vehicle model was used for controller development, and a 2D nonlinear model was developed for controller validation. The control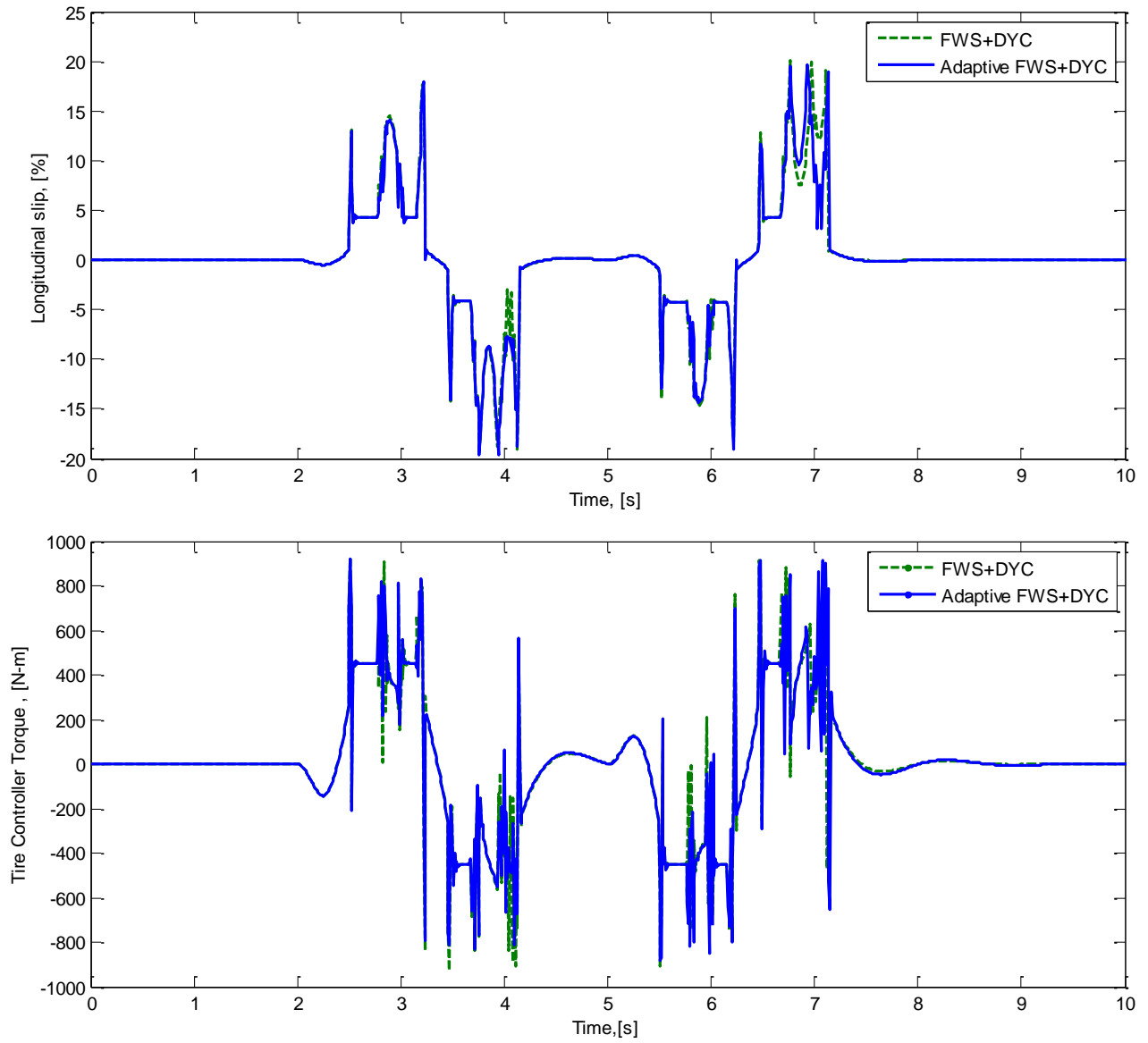ler was validated for a low friction, double lane change maneuver with uncertainty in the vehicle parameters. Improvements to the control scheme were proposed such as filtering the yaw moment output of the high level controller to reduce the required motor torque.

The results of these simulations indicate that the adaptive parameter estimates did not meaningfully improve the system response, as both control by combined FWS+DYC and control by 4WS were able to stabilize the vehicle in the presence of significant parameter changes. Furthermore, the adaptive controller increases the complexity of the system and adds additional failure modes in the form of unbounded parameter estimates. Though it can't be seen directly in the results, the differential equations being solved are very stiff and require a very small time step to successfully calculate. This may present further implementation difficulties in an actual system, as a very fast processor would be required.

The conclusions drawn in [Mirzaei, 2010] appear to be particularly relevant to the work presented here, as minimizing the yaw moment intervention would likely improve controller response. The ideal VSC system would exert minimal controller intervention when needed, and likely only intervene when the vehicle begins to demonstrate unstable behavior.

Design of an effective VSC system must also account for vehicle wear and passenger comfort. The DYC controller was improved by filtering the yaw output of the controller, but concerns still arise about the rapidly changing motor torques and its effect on motor life. An attempt was made at filtering the commanded torque from the tire slip controller, but it was found to be ineffective when implemented both with and without the yaw moment filter.

Additional study should be performed using a more complex motor model and tire slip controller.

Several challenges were faced in developing an appropriate model reference stability controller. In particular, with the controller derivation implemented in this paper there is no general technique for tuning the controllers, and different selections for $A_m$ and $Q$ can give wildly differing results. When tire force limitations were neglected in the linearized case, nearly any combination of $A_m$ and $Q$ gave satisfactory results. However, when the tractive limits of the tires were reached in the nonlinear simulations, the elements of the selected matrices were restricted to significantly smaller values. At high gains the system exhibited poor tracking performance and occasionally drove the vehicle to instability. When the controller gains are kept small, the controller intervention remains within a physically realizable bound. Proper tuning was also found to be difficult on the parameter updates when implementing an adaptive controller. When the values of K and L are calculated, it is found that the elements vary in size by several orders of magnitude. It is very challenging to find an appropriate set of controller gains that are large enough to cause meaningful changes in the largest of terms without generating extreme variations in the smallest. Another difficulty faced by the combined FWS and DYC controller is the excessive torque required to achieve the desired tire longitudinal slip. Even when the torque is limited to a reasonable value, the frequency of the required torque is still large, and could cause excessive wear on the tires and motor. It is possible that there exists a tuning that would avoid these problems, but one could not be found.

Controller validation would benefit from an improved vehicle and driver model. In the results presented, the driver steering angle was based on a simple scheduled steering wheel angle. While this worked in the majority of cases tested, certain cases like the low friction double lane change with parameter error would benefit from the addition of a driver model. A driver model could indicate whether or not performance could be recovered through proper driver intervention, and may also lend insight into how the controller would affect the driving experience. Simulating the effect of suspension and load transfer would also be a valuable

study, as they would cause further deviations from the linear model. Inclusion of a valid actuator model and tire slip controller is critical in evaluating the performance of a DYC controller. Without accounting for motor dynamics, it is easy to design a controller that is not physically realizable by any production vehicle.

Overall, the four wheel steering approach proved to be the most attractive form of control due to its effectiveness and simplicity of implementation. Even with uncertain parameters, the controller stabilized the vehicle while maintaining a high yaw rate and low slip angle. The DYC approach, though effective in stabilizing the vehicle in low friction conditions, led to a marked decrease in vehicle yaw rate and could potentially decrease motor life due to the rapidly changing torque commands. In both cases, though system velocity remains largely unaffected, the yaw rate is decreased from the un-controlled case in previously safe driving conditions. This decrease could give the driver the impression that the car is less responsive with control than without. It is possible that this could be overcome with a different reference model.

Though the technique presented for adaptive control was found to be ineffective, numerous other techniques exist such as adaptive pole placement, ANFIS, and immersion and invariance. Furthermore, robustness modifications were not pursued, and could be used to prevent problems such as parameter drift. Additional research could also be pursued in actuator rate limited control. By limiting the rate of change of the desired yaw moment, the required torque might be reduced into a realizable range.

# Glossary

| | |
|---|---|
| 4WS | Four Wheel Steering |
| ABS | Antilock Braking System |
| $C_f$ | Front wheel cornering stiffness |
| $C_r$ | Rear wheel cornering stiffness |
| DYC | Direct Yaw Control |
| ESP | Electronic Stability Program |
| FWS | Front Wheel Steering |
| $I_z$ | Moment of inertia about the c.g. |
| $L_f$ | Distance from c.g. to front axle |
| $L_r$ | Distance from c.g. to rear axle |
| M | Vehicle mass |
| MIMO | Multi Input, Multi Output |
| MRAC | Model Reference Adaptive Control |
| RWS | Rear Wheel Steer |
| SISO | Single Input, Single Output |
| TCS | Traction Control System |
| $\beta$ | Vehicle side slip angle |
| $\delta$ | Tire steering angle |
| $\Psi$ | Vehicle angle |
| $\Omega$ | Vehicle rotation rate |
| $\mu$ | Coefficient of road friction |

# References

[Abe, et al., 2001] Abe, Masato, et al. "Side-slip control to stabilize vehicle lateral motion by direct yaw moment." JSAE review 22.4 (2001): 413-419.

[Akella, 2013] Akella, Maruthi R. ASE 396 System ID and Adaptive Controls: Class Notes. University of Texas at Austin, 2013

[Canudas & Tsiotras, 1999] de Wit, Carlos Canudas, and Panagiotis Tsiotras. "Dynamic tire friction models for vehicle traction control." (1999).

[Canudas, et al., 2003] Canudas-de-Wit, Carlos, et al. "Dynamic friction models for road/tire longitudinal interaction." Vehicle System Dynamics 39.3 (2003): 189-226.

[Furukawa & Abe, 1997] Furukawa, Yoshimi, and Masato Abe. "Advanced chassis control systems for vehicle handling and active safety." Vehicle System Dynamics 28.2-3 (1997): 59-86.

[Hsiao, 2013] Hsiao, Tesheng. "Direct longitudinal tire force control under simultaneous acceleration/deceleration and turning." American Control Conference (ACC), 2013. IEEE, 2013.

[Iannou & Sun, 2012] Ioannou, Petros A., and Jing Sun. Robust adaptive control. Courier Dover Publications, 2012.

[Jianyong, et al., 2007] Jianyong, Wu, et al. "Improvement of vehicle handling and stability by integrated control of four wheel steering and direct yaw moment." Control Conference, 2007. CCC 2007. Chinese. IEEE, 2007.

[Kahveci, 2009] Nazli E. Kahveci (2009). Adaptive Control Design for Uncertain and Constrained Vehicle Yaw Dynamics, Frontiers in Adaptive Control, Shuang Cong (Ed.), ISBN: 978-953-7619-43-5, InTech

[Liang, et al., 2009] Liang, Wei, et al. "Vehicle pure yaw moment control using differential tire slip."American Control Conference, 2009. ACC'09.. IEEE, 2009.

[Liebermann, et al., 2004] Liebemann, E. K., et al. "Safety and performance enhancement: the Bosch electronic stability control (ESP)." SAE Paper 20004 (2004): 21-0060.

[Longoria, 2013] Longoria, Raul G. ME 390 Vehicle Dynamics: Class Notes. University of Texas at Austin, 2013

[Mirzaei, 2010] Mirzaei, M. "A new strategy for minimum usage of external yaw moment in vehicle dynamic control system." Transportation Research Part C: Emerging Technologies 18.2 (2010): 213-224.

[Mokhiamar & Abe, 2002a] Mokhiamar, O., and Masato Abe. "Active wheel steering and yaw moment control combination to maximize stability as well as vehicle responsiveness during quick lane change for active vehicle handling safety." Proceedings of the Institution of Mechanical Engineers, Part D: Journal of Automobile Engineering216.2 (2002): 115-124.

[Mokhiamar & Abe, 2002b] Mokhiamar, Ossama, and Masato Abe. "Effects of model response on model following type of combined lateral force and yaw moment control performance for active vehicle handling safety." JSAE Review 23.4 (2002): 473-480.

[Ohara & Murakami, 2008] Ohara, Hiroki, and Toshiyuki Murakami. "A stability control by active angle control of front-wheel in a vehicle system." Industrial Electronics, IEEE Transactions on 55.3 (2008): 1277-1285.

[Pacejka & Besselink, 1997] Pacejka, H. B., and I. J. M. Besselink. "Magic formula tyre model with transient properties." Vehicle system dynamics 27.S1 (1997): 234-249.

[Pacejka, et al., 1987] Pacejka, Hans B., Egbert Bakker, and Lars Nyborg. "Tyre modelling for use in vehicle dynamics studies." SAE paper 870421 (1987).

[Protean, 2014] "Protean Drive Specifications." ProteanElectric.com. Protean Electric Specifications, n.d. Web. 7 Apr. 2014.

[Shino & Nagai, 2001] Shino, Motoki, and Masao Nagai. "Yaw-moment control of electric vehicle for improving handling and stability." JSAE review 22.4 (2001): 473-480.

[Steeds, 1960] Steeds, William. Mechanics of road vehicles: a textbook for students, draughtsmen and automobile engineers. Iliffe, 1960.

[Svendenius, 2007] Svendenius, Jacob. "Tire Modeling and Friction Estimation." Diss. Lund University, 2007. Web. 8 April. 2014.

[Uil, 2007] Uil, R. T. "Tyre models for steady-state vehicle handling analysis." Thesis. Eindhoven University of Technology, 2007. Web. 8 April. 2014.

[Van Zanten, 2002] Van Zanten, Anton T. "Evolution of electronic control systems for improving the vehicle dynamic behavior." Proceedings of the 6th International Symposium on Advanced Vehicle Control. 2002.

[Wang & Hsieh, 2009] Wang, Junmin, and Ming-Feng Hsieh. "Vehicle yaw-inertia-and mass-independent adaptive steering control." Proceedings of the Institution of Mechanical Engineers, Part D: Journal of Automobile Engineering 223.9 (2009): 1101-1108.

[Wang & Longoria, 2006] Wang, Junmin, and Raul G. Longoria. "Combined tire slip and slip angle tracking control for advanced vehicle dynamics control systems." Decision and Control, 2006 45th IEEE Conference on. IEEE, 2006.

[Wang, 2007] Wang, Junmin. "Coordinated and Reconfigurable Vehicle Dynamics Control." Diss. The University of Texas at Austin, 2007. Web. 8 April. 2014.

[Wong, 2001] Wong, Jo Yung. Theory of ground vehicles. John Wiley & Sons, 2001.

[Zheng & Anwar, 2009] Zheng, B., and S. Anwar. "Yaw stability control of a steer-by-wire equipped vehicle via active front wheel steering." Mechatronics 19.6 (2009): 799-804.

## Vita

Mathew Ward Bissonnette was born in California in 1989. He received his Bachelor of Science in Mechanical Engineering from The California Polytechnic State University in San Luis Obispo in 2012. He then entered The University of Texas at Austin as a Masters student in Fall 2012. After graduation in Spring 2014, he will be working as a Control Systems Engineer at The Aerospace Corporation.

E-mail: Mathew.Bissonnette@gmail.com

This thesis was typed by the author.